



澳門大學
UNIVERSIDADE DE MACAU
UNIVERSITY OF MACAU

Outstanding Academic Papers by Students

學生優秀作品



DESIGN AND IMPLEMENTATION OF A RIDE HEIGHT CONTROL
SYSTEM FOR A QUARTER CAR WITH ACTIVE AIR
SUSPENSION

by

Chan Sio Hong

Ian Wai Fan

B.Sc. in Electromechanical Engineering

2016



Faculty of Science and Technology
University of Macau

Design And Implementation Of A Ride Height Control System For A Quarter Car

With Active Air Suspension

by

Chan Sio Hong (D-B2-2811-8)

Ian Wai Fan (D-B2-2808-8)



Faculty of Science and Technology

University of Macau

2016

University of Macau

Abstract

Design And Implementation Of A Ride Height Control System For A Quarter Car

With Active Air Suspension

by

Chan Sio Hong (D-B2-811-8)

Ian Wai Fan (D-B2-2808-8)

Project Supervisor
Prof. Wong Pak Kin

Department of Electromechanical Engineering, Faculty of Science and Technology

The active air suspension system has drawn recently the attention from the vehicle manufacturer because it can improve the stability of the vehicles and ride comfort by adjusting the ride height. Due to the nonlinear characteristics of air, it is very hard to regulate the ride height to the target value accurately. This project proposes an inflatable air spring to adjust the ride height in order to achieve a good ride handling capacity. In this project, a nonlinear mathematical model for a quarter car model with active air suspension and an air charging and discharging model are

constructed. These models are used to design a suitable control method and verify the feasibility of the control methods. Comparisons among different control methods, such as feedback control method, fuzzy control and reference model method, are made.

The simulation results show that the performance is good under a suitable control method. In other words, the adjustment of the ride height can be finished within an acceptable speed and an acceptable precision can be obtained. Eventually, fuzzy controller is selected to implement to the ride height control (RHC) system by comparing the simulation results.

Furthermore, a RHC system is designed and implemented on a quarter car test rig (QCTR). A series of experimental results are used to verify the functionality of the RHC system.

ACKNOWLEDGEMENTS

The authors wish to thank the supervisor, Prof. Wong Pak Kin, for his patient instruction, constructive guidance and valuable comments. The authors would also like to thank Mr. Zhao Jing and Mr. Zhao Rongchen for their assistance with experiment setup and their precious help in the development of the control algorithm and the implementation of the system. Without the support and encouragement from them, the authors cannot make the completion and success of this project.

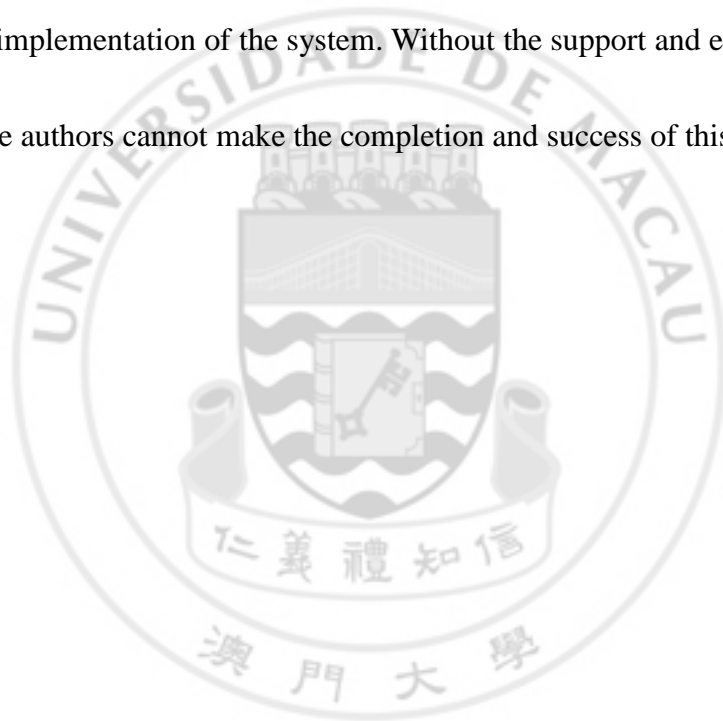


TABLE OF CONTENT

List of tables	a
List of figures	b
List of abbreviation.....	f
Nomenclature	g
Chapter 1: Introduction.....	1
1.1 General background.....	1
1.2 Background on active suspension system	2
1.3 Literature review	3
1.4 Project objectives.....	5
Chapter 2: Modeling of air suspension system.....	7
2.1 Modeling of air suspension system	9
2.1.1 Passive air spring model.....	9
2.1.2 Damper model	10
2.2 Air charging and discharging model	11
2.3 Quarter car model.....	12
Chapter 3: Design of control method for ride height control system	14
3.1 Static ride height control with feedback control method.....	15
3.1.1 Control concept	15
3.1.2 Construction of simulation	16
3.1.3 Result of charging process.....	18
3.1.4 Result of discharging process	20
3.2 Static ride height control with fuzzy controller	22
3.2.1 Control concept	22

3.2.2 Construction of simulation	24
3.2.3 Result of charging process.....	25
3.2.4 Result of discharging process.....	28
3.3 Static ride height control with reference model method	31
3.3.1 Control concept	31
3.3.2 Construction of simulation	33
3.3.3 Result of charging process.....	35
3.3.4 Result of discharging process.....	37
3.4 Discussion of simulation results.....	40
Chapter 4: Implementation of the ride height control system.....	44
4.1 Construction of the ride height control system.....	44
4.1.1 Air tank system.....	47
4.1.2 Air charging and discharging system	47
4.2 Signal processing devices and software	50
4.2.1 Data acquisition and processing	51
4.2.2 Control software.....	53
4.3 Air suspension system and quarter car test rig	54
4.3.1 Inflatable air spring system	55
4.3.2 Quarter car test rig.....	56
Chapter 5: Experimental results	58
5.1 Static ride height control with fuzzy controller.....	58
5.1.1 Result of charging process.....	58
5.1.2 Result of discharging process.....	61
5.2 Discussion of experimental results.....	63
Chapter 6: Conclusions.....	64
6.1 Summary.....	64

6.2 Originalities	65
6.3 Recommendation for future work	65
Reference	67
Appendix I: Work breakdown	71



LIST OF TABLES

<i>Number</i>	<i>Page</i>
Table 3.1 Input parameter for quarter car model.....	14
Table 3.2 Rule of fuzzy controller.....	23
Table 3.3 Summary of simulation results of charging processes	42
Table 3.4 Summary of simulation results of discharging processes	42
Table 4.1 Specification of air compressor.....	47
Table 4.2 Specification of the solenoid valve	49
Table 4.3 Specification of displacement sensor	49
Table 4.4 Specification of air pressure sensor.....	49
Table 4.5 Specifications of NI module: NI 9215	52
Table 4.6 Specifications of NI module: NI 9401	52
Table 4.7 Specifications of NI chassis: cDAQ-9178	53

LIST OF FIGURES

<i>Number</i>	<i>Page</i>
Figure 2.1 Schematic diagram of ACDC system	7
Figure 2.2 Block diagram of the pneumatic circuit.....	8
Figure 3.1 Flow chart of static ride height control with feedback control method.....	15
Figure 3.2 Construction of simulation of static ride height control with feedback control method.....	16
Figure 3.3 Simulation result of charging process with feedback control method - displacement of the sprung mass.....	18
Figure 3.4 Simulation result of charging process with feedback control method - gauge pressure inside the air spring.	19
Figure 3.5 Simulation result of charging process with feedback control method - mass of air changed inside the air spring	19
Figure 3.6 Simulation result of charging process with feedback control method - control command.....	20
Figure 3.7 Simulation result of discharging process with feedback control method -displacement of sprung mass	20
Figure 3.8 Simulation result of discharging process with feedback control method - gauge pressure inside the air spring.	21
Figure 3.9 Simulation result of discharging process with feedback control method - mass of air changed inside the air spring.	21
Figure 3.10 Simulation result of discharging process with feedback control method - control command.	22

Figure 3.11 Construction of static ride height control with fuzzy controller	24
Figure 3.12 Simulation result of charging process with fuzzy controller - displacement of the sprung mass.....	25
Figure 3.13 Simulation result of charging process with fuzzy controller - gauge pressure inside the air spring.....	26
Figure 3.14 Simulation result of charging process with fuzzy controller - mass of air changed inside the air spring.....	26
Figure 3.15 Simulation result of charging process with fuzzy controller - control command	27
Figure 3.16 Simulation result of charging process with fuzzy controller - duty cycle	27
Figure 3.17 Simulation result of discharging process with fuzzy controller - displacement of the sprung mass.....	28
Figure 3.18 Simulation result of discharging process with fuzzy controller - gauge pressure inside the air spring.....	29
Figure 3.19 Simulation result of discharging process with fuzzy controller - mass of air changed inside the air spring	29
Figure 3.20 Simulation result of discharging process with fuzzy controller - control command.....	30
Figure 3.21 Simulation result of discharging process with fuzzy controller - duty cycle.	30
Figure 3.22 Flow chart of static ride height control with reference model	32
Figure 3.23 Construction of static ride height control with reference model method.....	33
Figure 3.24 Simulation result of charging process with reference model method - displacement of the sprung mass.....	35

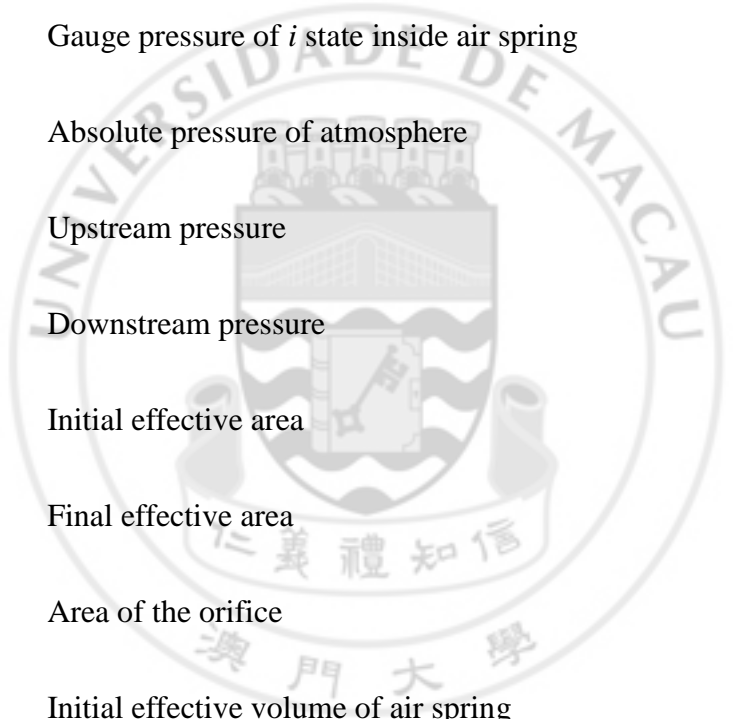
Figure 3.25 Simulation result of charging process with reference model method - gauge pressure inside the air spring	35
Figure 3.26 Simulation result of charging process with reference model method - mass of air changed inside the air spring	36
Figure 3.27 Simulation result of charging process with reference model method - control command.....	36
Figure 3.28 Simulation result of charging process with reference model method - duty cycle	37
Figure 3.29 Simulation result of discharging process with reference model method - displacement of the sprung mass	37
Figure 3.30 Simulation result of discharging process with reference model method - gauge pressure inside the air spring.....	38
Figure 3.31 Simulation result of discharging process with reference model method - mass of air changed inside the air spring.....	38
Figure 3.32 Simulation result of discharging process with reference model method - control command	39
Figure 3.33 Simulation result of discharging process with reference model method – duty cycle	39
Figure 4.1 Overview of ride height control system.....	44
Figure 4.2 Block diagram of interconnection among the QCTR, RHC system and control and data acquisition hardware.....	46
Figure 4.3 Illustration of solenoid valves.....	48
Figure 4.4 Overview of the quarter car test rig with sensors	54
Figure 4.5 Rear view of the QCTR	56
Figure 4.6 Positions of the sensors and the structure of the suspension system	57

Figure 5.1 Experimental result of charging process with fuzzy controller - displacement of the sprung mass.....	58
Figure 5.2 Experimental result of charging process with fuzzy controller - gauge pressure inside the air spring.....	59
Figure 5.3 Experimental result of charging process with fuzzy controller – amount of mass of air inside the air spring	59
Figure 5.4 Experimental result of charging process with fuzzy controller - control command	60
Figure 5.5 Experimental result of discharging process with fuzzy controller - displacement of the sprung mass.....	61
Figure 5.6 Experimental result of discharging process with fuzzy controller - gauge pressure inside the air spring	61
Figure 5.7 Experimental result of discharging process with fuzzy controller – amount of mass of air inside the air spring	62
Figure 5.8 Experimental result of discharging process with fuzzy controller - control command.....	62

LIST OF ABBREVIATION

ECAS	Electronic controlled air suspension
QCTR	Quarter car test rig
ACDC	Air charging and discharging system
PWM	Pulse width modulation
VSC	Variable Structure Control
RHC	Ride height control
SMC	Sliding mode control
PID	Proportional-Integral-Derivative
MPC	Model predictive control

NOMENCLATURE



P_0	Initial gauge pressure inside air spring
P_e	Final gauge pressure inside air spring
P_{i-1}	Gauge pressure of $i-1$ state inside air spring
P_i	Gauge pressure of i state inside air spring
P_{atm}	Absolute pressure of atmosphere
P_{up}	Upstream pressure
P_{dn}	Downstream pressure
A_0	Initial effective area
A_e	Final effective area
A_{ori}	Area of the orifice
V_0	Initial effective volume of air spring
V_e	Final effective volume of air spring
V_{i-1}	Effective volume of $i-1$ state of air spring
V_i	Effective volume of i state of air spring
α	Coefficient of variation of effective volume
β	Coefficient of variation of effective area

C_s	Viscous damping coefficient
z_s	Displacement of sprung mass
z_u	Displacement of unsprung mass
\dot{z}_s	Rate of change of displacement of sprung mass
\dot{z}_u	Rate of change of displacement of unsprung mass
$q_{air,in}$	Mass flow rate of air flows into air spring
$q_{air,out}$	Mass flow rate of air flows out from air spring
κ	Polytropic index
R	Perfect gas constant
T_t	Internal temperature of the air tank
M_{air}	Total change of air mass inside the air spring
m_{air}	Change of air mass inside the air spring in a single cycle
m_s	Sprung mass
m_u	Unsprung mass

CHAPTER 1: INTRODUCTION

This chapter serves as an introductory overview of the project. The background of the project is briefly studied, followed by a literature review related to the project scope. The objective of the project is also given at the end of this chapter.

1.1 GENERAL BACKGROUND

The development of the transportation industry tends to concern more about commercial vehicles [1, 2]. As one of the most important parts of vehicles, suspension system is responsible to provide ride comfort and handling capacity by adjusting vehicle height and level [3, 4]. The suspension system consists of tires, springs, shock absorbers and linkages that connect a vehicle to its wheels. The traditional passive suspension provides a fixed characteristics such as constant stiffness and damping. However, ever-increasing demand of the vehicle performance determines that the traditional passive suspension system cannot meet the advances of the vehicles, such as vehicle ride height control, adjustable damping force control, etc. In order to satisfy the raising requirement, an active suspension system can be applied to vehicles. It is used to adjust the ride height to the target value, and hence a good driving stability, ride comfort and fuel economy can be achieved even the pavement varies frequently [3, 5-7].

1.2 BACKGROUND ON ACTIVE SUSPENSION SYSTEM

There are many types of active suspension systems, such as hydraulic suspension system, hydropneumatic suspension system and air suspension system, available in commercial vehicles.

The hydraulic systems are the most prevalent type of suspension leveling systems in commercial vehicles. In 1996, a hydraulic ride height control system for a race track is developed by J. Braun [8]. However, the pumps are needed to be activated every time when the ride height is needed to be adjusted. It means that energy is consumed in every adjustment. Furthermore, the fixtures of hydraulic systems are massive because it is a closed circuit and the fluid is needed to be stored on the vehicles. Eventually, the vehicles will be laden after the installation and the suspension system are under a relatively large loading though the passengers still have not got on the vehicle.

Another common type of suspension leveling systems is the hydro-pneumatic system [9, 10]. The system takes advantages of the characteristics of fluid and gas. Due to the compressibility, the gas in the system acts as the springing medium and it has the same role as the helical spring of traditional suspension systems. Meanwhile, the fluid acts as a medium of damping and leveling. The system provides a soft and

comfortable ride handling capacity. However, the system is constructed with a complex construction. It means that it needs to take more time and manpower to install the system. Moreover, the pneumatic circuit and the hydraulic circuit are closed circuits. It is necessary to check and refill medium regularly to prevent leakages. Moreover, the problems in the hydraulic system still exists. They are the difficulties and inconvenience of construction and maintenance.

Rather than the two types of systems mentioned above, electronic controlled air suspension (ECAS) system is aimed to be studied in this report. The ECAS regulates the ride height by controlling the air mass inside the air spring and the regulating approach is to control the states of the solenoid valve [5, 11]. Therefore, ECAS system is a low-cost method to achieve the ride height control.

However, there are some problems existed in the control of the air suspension system, such as the complexity of the control system, nonlinear characteristics of air due to the compressibility and uncertainties mainly caused by payload variations [12]. In the case of these problems, the air compressibility may cause significant vertical oscillation, which seriously reduces the operation lifespan of the solenoid valve and deteriorate the vehicle dynamic performance [12-17].

1.3 LITERATURE REVIEW

In order to track the ride height and satisfy the control demand, some air charging

and discharging (ACDC) circuits and robust air suspension control strategies have been developed to solve the aforementioned problems. In the recent literature, several control approaches for a simple and generic pneumatic servo system were proposed, such as using a fuzzy gain scheduler based on local linear models [13, 15], neural network approach for switching control, backstepping control [17-19] and sliding mode control [12, 17-19]. Although these studies presented many advanced control technology, they were complex and the system performance cannot not be guaranteed in an analytical way. H. Kim and H. Lee developed sliding mode approach to carry out the ride height control in 2011 [20]. A Pulse width modulation (PWM) method was used to effectuate the control signal in this type of control strategy. According to their study, a mathematical model is constructed to predict the dynamic characteristic of a vehicle. A sliding mode control algorithm was developed to increase the tracking accuracy and supplemented the unpredictability and uncertainties of the mathematical model of the air suspension system. A sliding mode observer was also developed to evaluate the pressure inside the air spring.

However, Kim did not consider a condition with the random road disturbance. X. Xu, L. Chen, L. Q. Sun and X. D. Sun developed a dynamic ride height controller which was applied under a condition with random road disturbances [21]. A mathematical model of RHC system of a quarter car was established with the random

road excitation as a stochastic nonlinear system. The RHC system was decoupled using the differential geometry and a Variable Structure Control (VSC) strategy is used to stabilize the RHC system. However, some problems still need to investigate in ECAS systems. For example, the air-charging and discharging-mechanism of the ECAS system, as well as the integration of the inflatable air spring with the whole vehicle model.

1.4 PROJECT OBJECTIVES

According to the problems mentioned in the previous section, the first objective is the construction of a nonlinear mathematical model for a quarter car with active air suspension system. The selection of quarter car model is due to the availability of the QCTR in our automotive engineering laboratory. Comparisons between different types of control strategies are important to obtain the best one. In order to obtain the results of the systematically rather than trial and error, a simulated model is desired to estimate the ride height level and the corresponding mass of air. Furthermore, an ACDC model is needed to estimate the amount of air mass which flows into or out from the air spring. These models can also be the approximation of the state of a vehicle and it can be used as a model of prediction in some kinds of control strategies.

The second objective is to design a suitable control strategy for the RHC system. A control method is necessary to achieve a good performance in ride height

adjustments. To achieve this objective, one intelligent and model-free control approach, a fuzzy logic, and reference model method are developed and examined. Afterwards, a suitable control strategy can be chosen to implement the RHC system.

Besides the control methods, experimental results are essential to verify the functions of the chosen method. Therefore, the third objective is the design and the implementation of a RHC system for a quarter car with an air suspension. An ACDC system and an air tank system are involved. The key point for achieving this objective is the construction of the pneumatic circuit and electronic control circuit. The signal types of sensors, the properties of the QCTR and the pneumatic suspension system and the connections among the QCTR, the pneumatic circuit and the electronic control circuit are required to be truly determined in order to build up the experiment. Moreover, data acquisition system and data processing program, such as National Instrument devices (NI), LabVIEW program, VeriStand program and MATLAB program, must be studied in details in order to accomplish in the experiments.

CHAPTER 2: MODELING OF AIR SUSPENSION SYSTEM

This chapter covers about the equations used in modeling of the air suspension system. It consists of an air spring model and a constant damper model. Moreover, an ACDC model and a quarter car model are constructed in order to build up simulated model of ACDC system for a quarter car with air suspension.

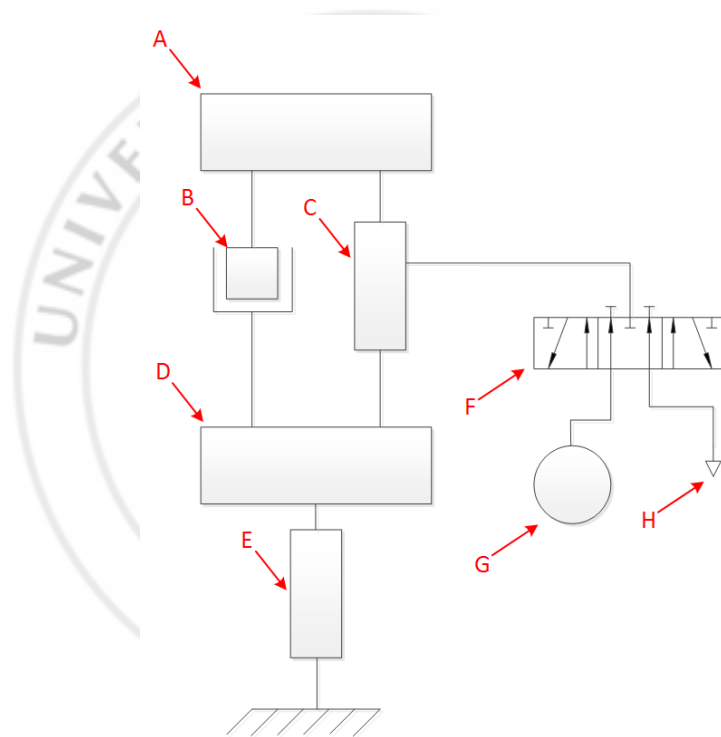


Figure 2.1 Schematic diagram of ACDC system

Figure 2.1 shows the scheme of the ACDC system. The components are listed as following:

- A. Sprung mass
- B. Constant damper

C. Inflatable air spring

D. Unprung mass

E. Wheel

F. Solenoid valve

G. Air tank

H. Atmosphere

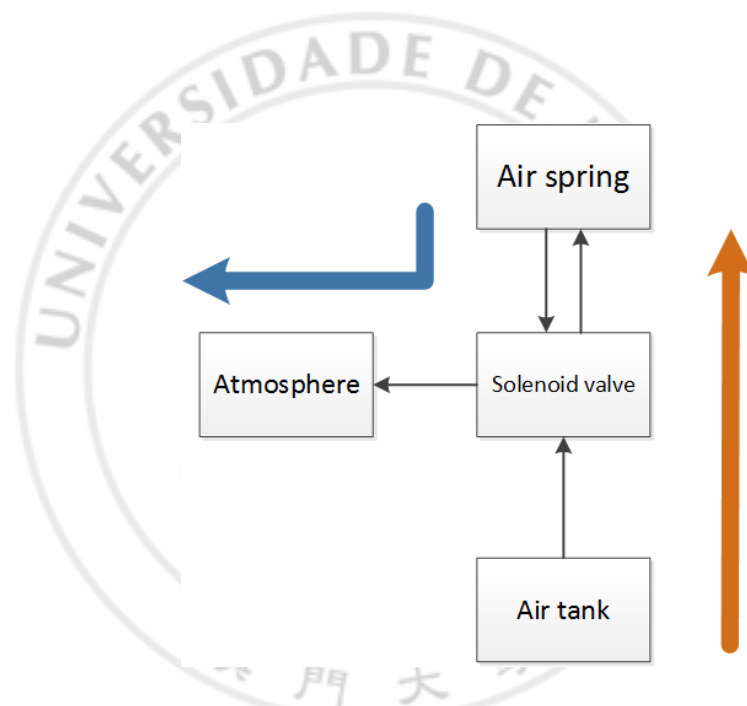


Figure 2.2 Block diagram of the pneumatic circuit

Figure 2.2 shows the construction of the pneumatic circuit. The brown arrow represents the route of air flow in charging process. Firstly, the compressed air is stored in an air tank. When the charging process is being executed, the solenoid valve switch on and the air flows through the valve into the air spring. The blue arrow represents the route of air flow in discharging process. When the discharging process

is being executed, the air in the air spring flows through the valve to the atmosphere.

2.1 MODELING OF AIR SUSPENSION SYSTEM

The following assumptions are made for the models:

- (1) The air spring model is created on the basis of thermodynamics and ideal gas law.
- (2) The time spent in every single period of charging and discharging process is very short. There is not enough time for heat transfer between the air spring and the environment. Therefore, it is regarded as an adiabatic and isothermal process.
- (3) The air reservoir is considered as a constant gas resource with a fixed volume.
- (4) The energy loss of air in the air spring and the plumbing components is negligible.

2.1.1 Passive air spring model

The equation below can be obtained from the Boyle's law

$$(P_0 + P_{atm})V_0^\kappa = (P_e + P_{atm})V_e^\kappa \quad (1)$$

where P_0 is the initial gauge pressure inside the air spring, P_e is the final gauge pressure inside the air spring, P_{atm} is the atmospheric pressure, V_0 is the effective volume of the initial state, V_e is the effective volume of the final state and κ is the polytropic index.

As the air spring is being deformed caused by the charging and discharging process, the increasing of the load of the vehicle, etc., the instantaneous effective area and volume are varied by the length of the air spring. They can be described as follows:

$$V_e = V_0 + \alpha(z_s - z_u) \quad (2)$$

$$A_e = A_0 - \beta(z_s - z_u) \quad (3)$$

where A_0 is the effective area of the initial state A_e is the effective area of the final state, z_s is the displacement of the sprung mass, z_u displacement of the unsprung mass, α is the coefficient of variation of effective volume and β is the coefficient of variation of effective area. The unit of α and β are m^3/m and m^2/m respectively.

The force exerted by the air spring can be described as

$$F_{spring} = P_e A_e \quad (4)$$

2.1.2 Damper model

The damper is claimed as a constant damper. In other words, the force exerted by the damper is affected by the velocity of the deformation of the air spring. The expression of the force can be obtained as below:

$$F_{damper} = -C_s(\dot{z}_s - \dot{z}_u) \quad (5)$$

where C_s is the viscous damping coefficient, z_s is the displacement of the sprung mass and z_u is the displacement of the unsprung mass.

2.2 AIR CHARGING AND DISCHARGING MODEL

The mass flow rate of air flow through the solenoid valve can be obtained as below:

$$q_{air} = \begin{cases} \left(\frac{2}{\kappa+1} \right)^{\frac{\kappa+1}{2(\kappa+1)}} \sqrt{\frac{\kappa}{RT_i}} P_{up} A_{ori} & , P_{dn}/P_{up} < b \\ \left(\frac{2}{\kappa+1} \right)^{\frac{\kappa+1}{2(\kappa+1)}} \sqrt{\frac{\kappa}{RT_i}} P_{up} A_{ori} \sqrt{1 - \left(\frac{P_{dn}/P_{up} - b}{1-b} \right)^2} & , P_{dn}/P_{up} \leq 1 \end{cases} \quad (6)$$

where q_{air} is the mass flow rate of air that flows through the solenoid valve, κ is the polytropic index, R is the perfect gas constant, T_i is the temperature of the air reservoir, A_{ori} is the area of the orifice, P_{up} is the upstream pressure and P_{dn} is the downstream pressure. The values of P_{up} and P_{dn} depend on whether it is a charging or a discharging process. If it is a charging process, P_{up} is substituted by the absolute pressure of the air reservoir and P_{dn} is substituted by the instantaneous absolute pressure inside the air spring. Otherwise, P_{up} is substituted by the instantaneous absolute pressure inside the air spring and P_{dn} is substituted by the absolute pressure of atmosphere.

The total amount of change of air mass inside the air spring after the charging and discharging processes can be described as:

$$M_{air} = \int (q_{air,in} - q_{air,out}) dt \quad (7)$$

The equation of state can be obtained from thermodynamic theory because it is

a polytropic process with variable amount of mass:

$$R \cdot T_s \cdot M_{air} + (P_0 + P_{atm}) \cdot V_0^\kappa = (P_e + P_{atm}) \cdot V_e^\kappa \quad (8)$$

where M_{air} is the total amount of change of air mass inside the air spring and T_s is the internal temperature of the air spring.

Furthermore, it can be expressed as an equation in terms of the previous state and the present state as:

$$R \cdot T_s \cdot m_{air} + (P_{i-1} + P_{atm}) \cdot V_{i-1}^\kappa = (P_i + P_{atm}) \cdot V_i^\kappa \quad (9)$$

$$m_{air} = \int_0^t (q_{air,in} \cdot S_{in} - q_{air,out} \cdot S_{out}) dt \quad (10)$$

where m_{air} is the amount of change of air mass inside the air spring in every single cycle, t is the period of a cycle S_{in} and S_{out} are the signal of charging and discharging process respectively, P_{i-1} and V_{i-1} is the previous state of the air spring and P_i and V_i is the present state of the air spring.

After the adjustment begins, Eq. (1) is replaced by Eq. (9) and the model becomes an active air spring model.

2.3 QUARTER CAR MODEL

The following equations can be obtained by using Newton's Second Law to analyze the motion of sprung mass and the unsprung mass:

$$\begin{cases} m_s \ddot{z}_s = F_{spring} + F_{damper} + F_a \\ m_u \ddot{z}_u = F_{type} - F_{spring} - F_{damper} - F_a \end{cases} \quad (11)$$

From Eq. (11), if the active force is zero, the equations are obtained as:

$$\begin{cases} m_s \ddot{z}_s = F_{spring} + F_{damper} \\ m_u \ddot{z}_u = F_{wheel} - F_{spring} - F_{damper} \end{cases} \quad (12)$$

The force of a wheel can be treated as a type of spring with a constant spring coefficient. Therefore, it can be expressed as below:

$$F_{wheel} = k_w (z_s - z_u) \quad (13)$$

where k_w is the spring coefficient of wheel.



CHAPTER 3: DESIGN OF CONTROL METHOD FOR RIDE HEIGHT CONTROL SYSTEM

This chapter presents the concept and the construction of different control methods such as feedback control method, fuzzy controller and reference model method. Simulations are run and a series of simulation results are shown in this chapter for comparisons. The control method with the best performance is selected to implement to the RHC system. Table 3.1 shows the input parameter for the quarter car model.

Table 3.1 Input parameter for quarter car model

Parameter	Unit	Value
A_0	m^2	0.0095
A_{ori}	m^2	0.005
α	/	0.0207
b	/	0.528
β	/	0.0827
C_s	Ns/m	2000
κ	/	1.33
k_t	N/m	592000
m_s	kg	60

m_u	kg	30
P_0	Pa	175000
P_{atm}	Pa	101325
R	$Nm/(kg/k)$	287
T_s	K	293
T_t	K	293
V_0	m^3	6.6523×10^{-4}

3.1 STATIC RIDE HEIGHT CONTROL WITH FEEDBACK CONTROL

METHOD

3.1.1 Control concept

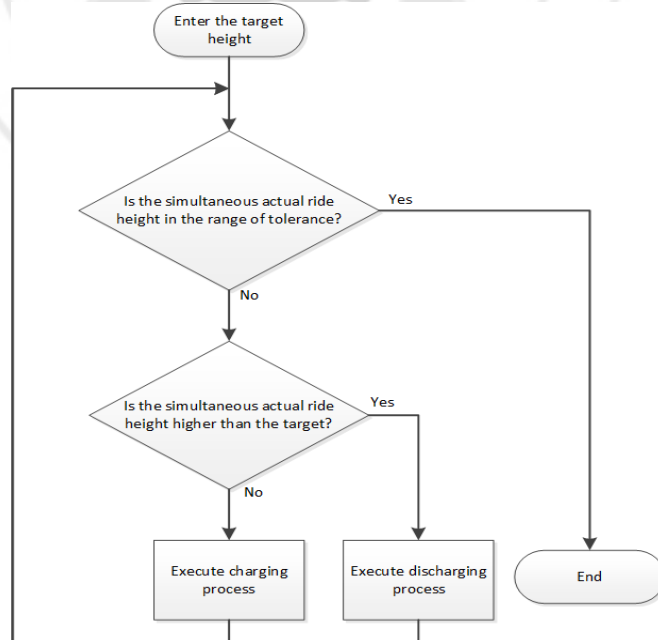


Figure 3.1 Flow chart of static ride height control with feedback control method

Figure 3.1 shows the control logic of feedback control method. It is a basic

concept of ride height adjustment. An acceptable range of tolerance is designed in this method. If the error is out of the range of tolerance, the system will judge whether it should be a charging or a discharging process until the error get into the range. The judgment depends on the sign of error. If the error is positive, which means that the target value is still higher than the actual height, a charging process is needed and vice versa. It only stops if the error is in the range of tolerance. The sample rate of the system is essential that it directly influences the result because the frequency of the judgment depends on the sample rate.

3.1.2 Construction of simulation

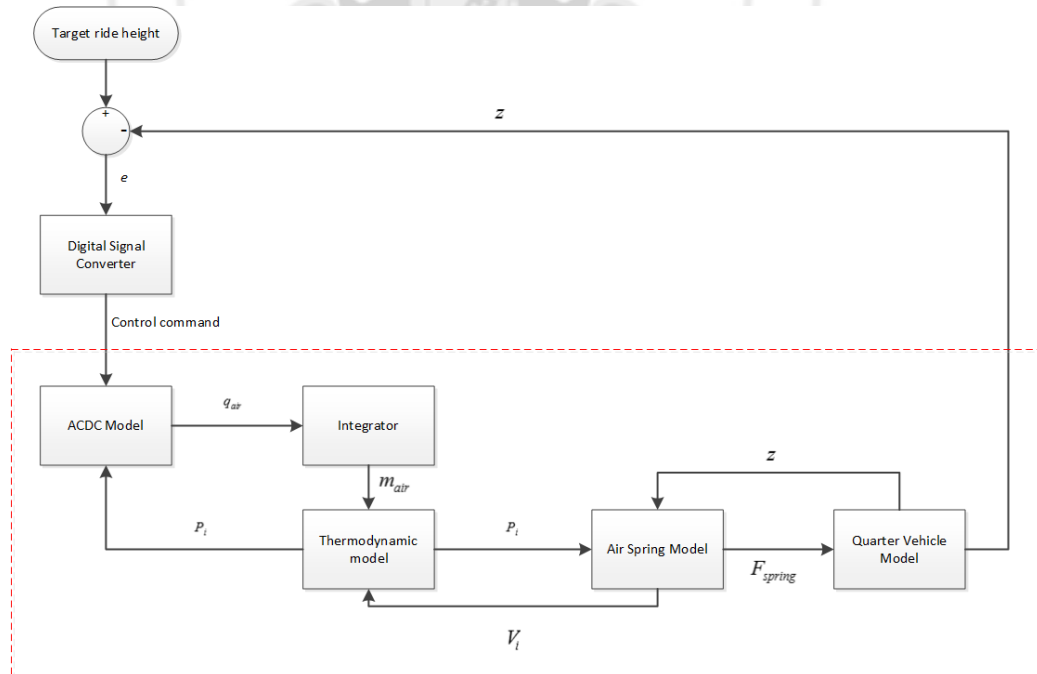


Figure 3.2 Construction of simulation of static ride height control with feedback control method

Figure 3.2 shows the configuration of the simulated model with feedback control

method. Firstly, the target value enters into the system and it will be compared with the instantaneous ride height. Afterwards, the error between them is produced and gets into the digital signal convertor. The convertor consists of a logic processor. Therefore, the value of error is put into this convertor and then a digital control signal is produced as the output to control the change of air mass inside the air spring. Then, the signal goes to ACDC model and control the amount of change of air mass inside the air spring.

After receiving the control signal, ACDC model calculates the amount of change of air mass and is transferred to the Thermodynamic model. Then the gauge pressure inside the air spring is calculated and transmitted to air spring model. The force is calculated in air spring model and transmitted to the quarter car model. Eventually, the motion of a quarter car is estimated and the ride height is transmitted back to the digital signal convertor. This is the signal flow of a cycle.

Additionally, in the first 0.2 seconds of the simulation, the air spring in the air suspension is treated as a passive air spring. In other words, ACDC model have not been activated yet and the action is occurred within the air spring model and the quarter car model only.

Afterwards, ACDC model and Thermodynamic model are activated. According to Eq. (9), P_i , P_{i-1} and V_{i-1} are required. P_{i-1}, V_{i-1} , P_i and V_i are substituted

by P_e and V_e which are from the air spring model at the instant of the start of the activation. After the cycle is done, the present gauge pressure inside the air spring, P_i , is transmitted to ACDC model. Furthermore, P_i and V_i are saved as P_{i-1} and V_{i-1} respectively in the Thermodynamic model for the next cycle.

The dotted region is the simulated model of an ACDC model and a quarter car model with air suspension. The Thermodynamic model is separated from the ACDC model mentioned in Section 2.2. It is built with Eq. (9) only. The reason of the separation is that the internal signal flow can be shown clearer.

3.1.3 Result of charging process

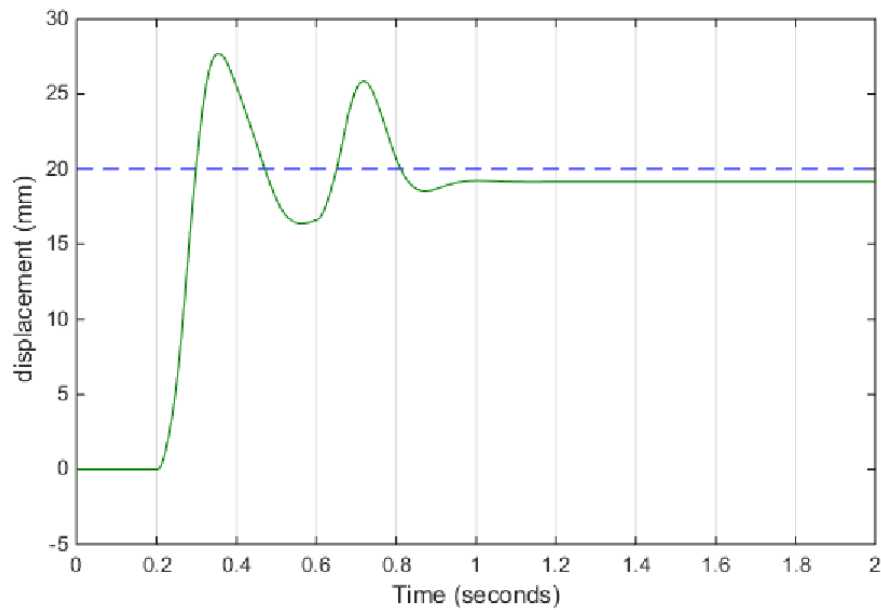


Figure 3.3 Simulation result of charging process with feedback control method - displacement of the sprung mass

In Figure 3.3, the blue dotted line is the target and green line is the actual one. It is obvious that the issue of overshooting is found and there are surplus because of over-

charging and over-discharging.

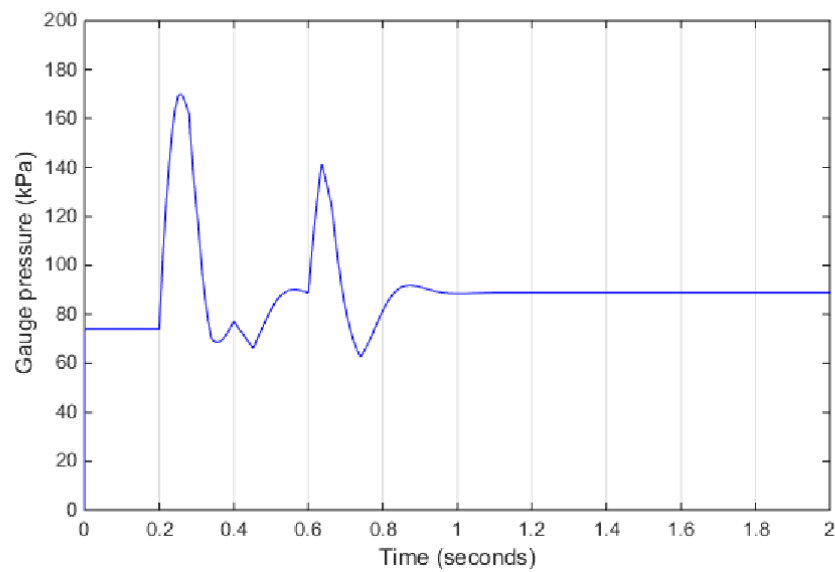


Figure 3.4 Simulation result of charging process with feedback control method - gauge pressure inside the air spring.

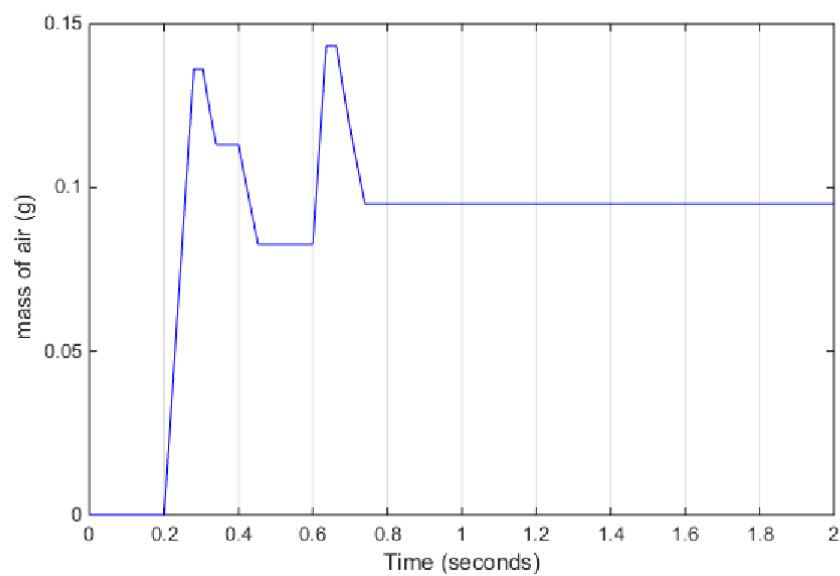


Figure 3.5 Simulation result of charging process with feedback control method - mass of air changed inside the air spring

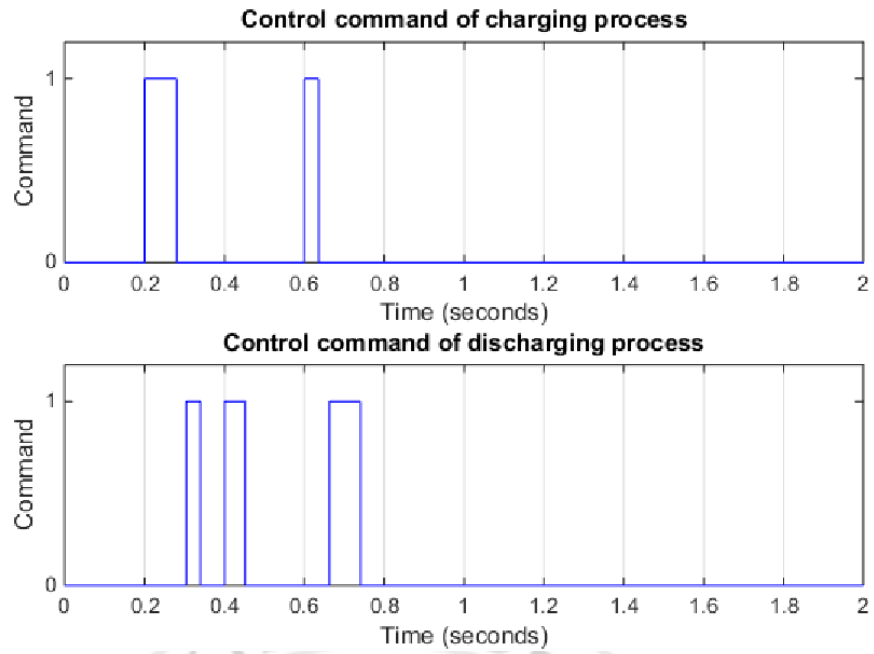


Figure 3.6 Simulation result of charging process with feedback control method -

control command

3.1.4 Result of discharging process

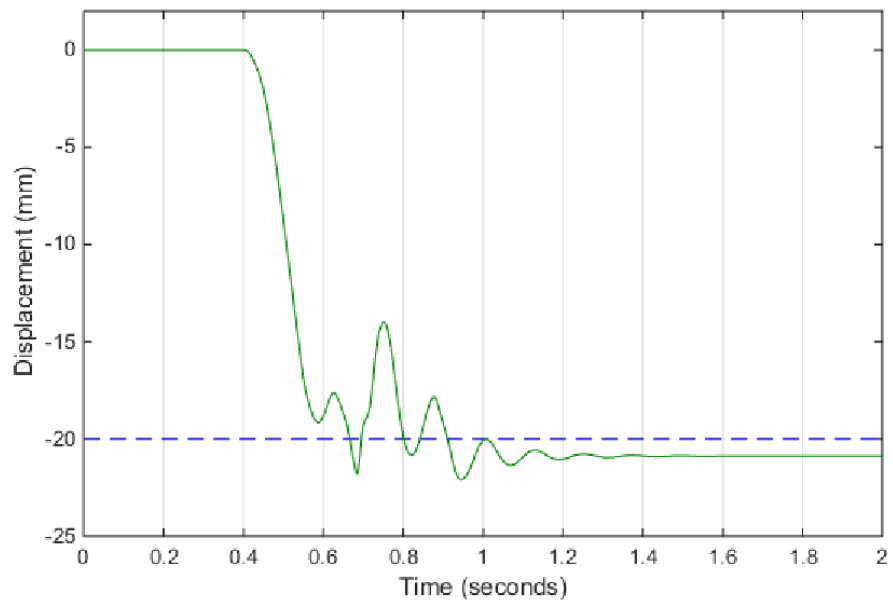


Figure 3.7 Simulation result of discharging process with feedback control method -

displacement of sprung mass

In Figure 3.7, the blue dotted line is the target and green line is the actual one.

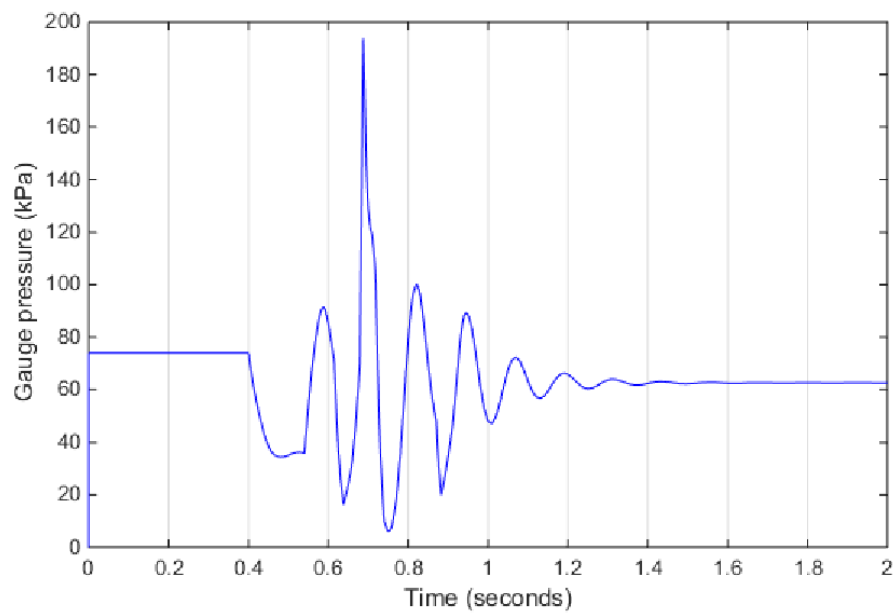


Figure 3.8 Simulation result of discharging process with feedback control method - gauge pressure inside the air spring.

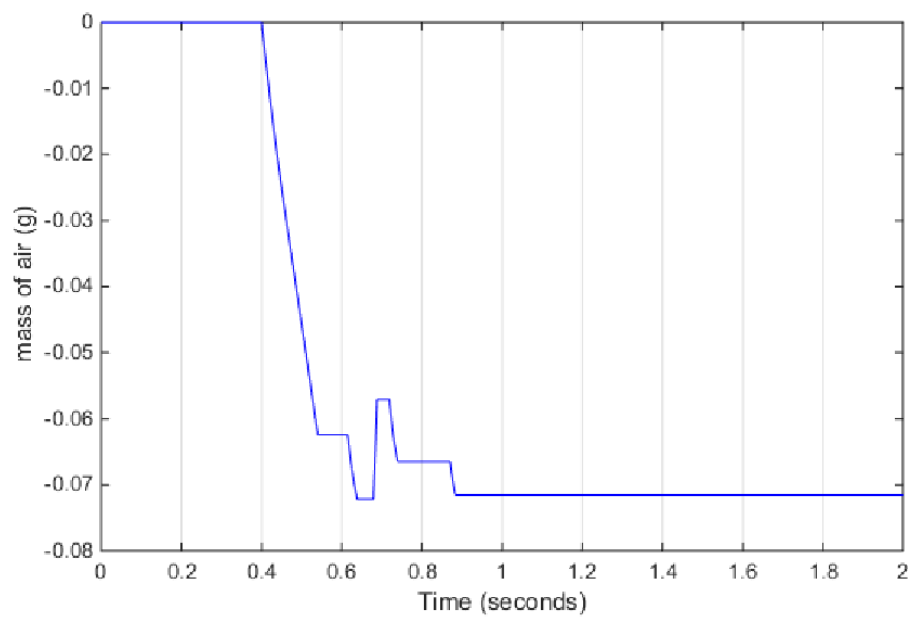


Figure 3.9 Simulation result of discharging process with feedback control method - mass of air changed inside the air spring.

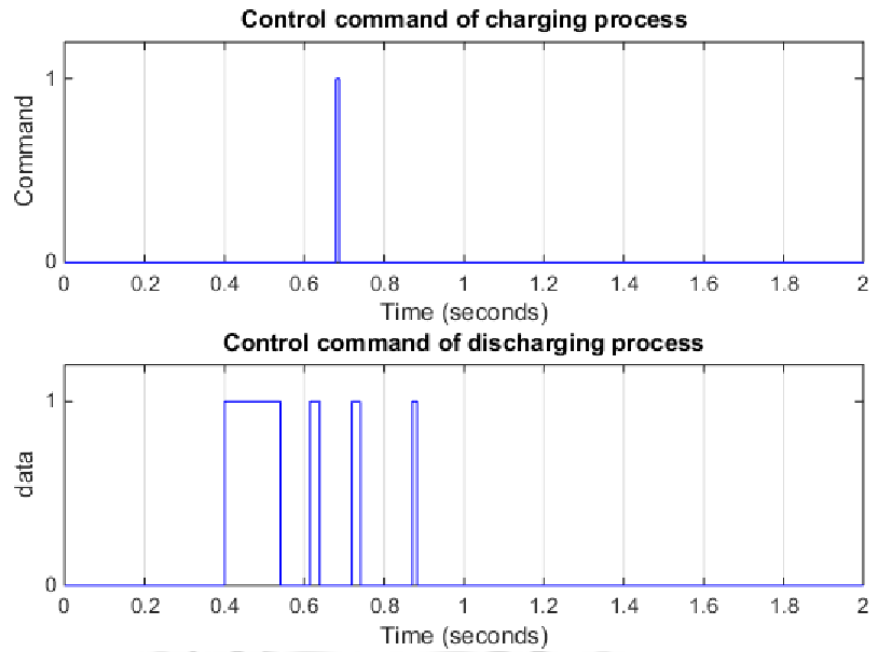


Figure 3.10 Simulation result of discharging process with feedback control method - control command.

3.2 STATIC RIDE HEIGHT CONTROL WITH FUZZY CONTROLLER

3.2.1 Control concept

In order to reduce overshooting, a controller is developed to control the speed of charging and discharging process. Fuzzy control method is decided to be used. Fuzzy controller is widely used due to its fast response and robustness.

As the working principle of the controller, the rate of change of the error, \dot{e} , and the error, e , are the inputs of the controller. Furthermore, duty cycles of PWM which is within a range from 0 to 1 are the outputs of the controller because the control command is executed by a series of PWM signal.

The Gaussian function is chosen as the membership function and the *if than else* rule is implemented to construct the relationship between the inputs and outputs. Table 3.2 shows the rules of the controller which are made of the engineer experience and trial and error.

Table 3.2 Rule of fuzzy controller

<i>Duty cycle</i>		\dot{e}		
		Small	Middle	Large
e	Large	Large	Middle	Middle
	Middle	Large	Middle	Middle
	Small	Small	Small	Small

3.2.2 Construction of simulation

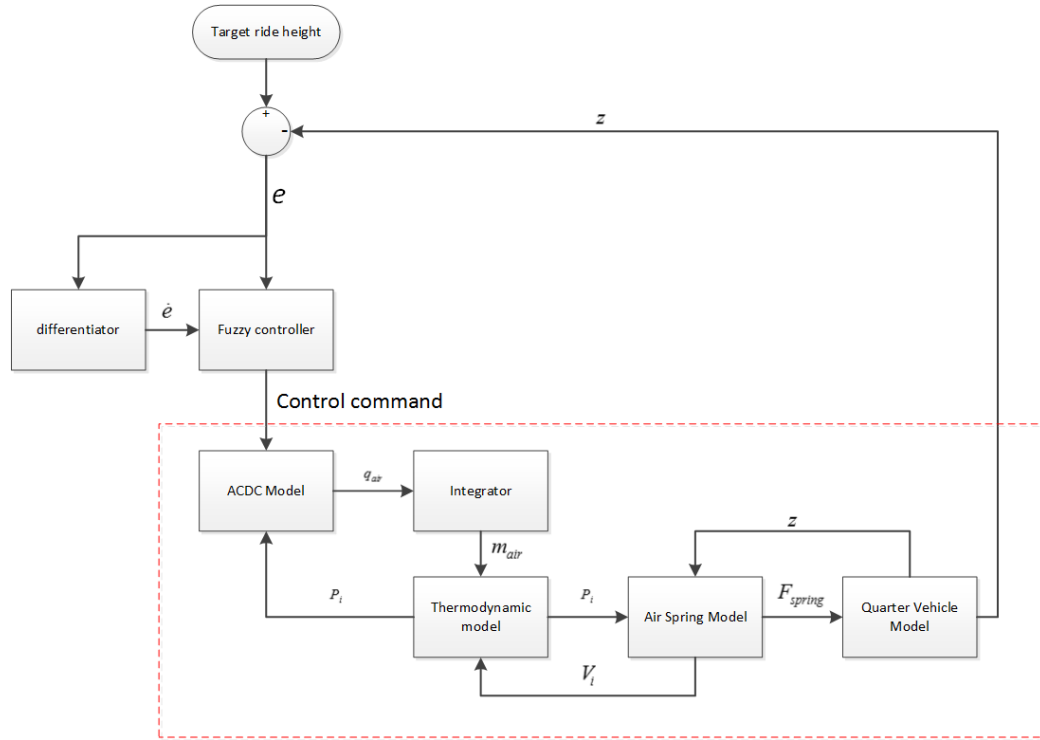


Figure 3.11 Construction of static ride height control with fuzzy controller

Figure 3.11 Construction of static ride height control with fuzzy controller shows the configuration of the simulation. After the target enters the system, it is also compared with the instantaneous ride height. The error and the rate of change of the error are fed to the fuzzy controller. It analyzes the inputs and produces duty cycles as output according the rules of fuzzy controller shown in Table 3.2 Rule of fuzzy controller. Different from the previous one, the ACDC model contains a PWM signal convertor, which can receive a signal of duty cycle and produce digital control signals as output. The instantaneous ride height is eventually adjusted and transmitted to compare with the target and the cycle is complete.

As an overview of the configuration, the difference between feedback control method and fuzzy controller is that the control output of fuzzy controller depends on the error and the rate of change of error but the feedback control method depends on the error only. The fuzzy controller can limit the amount of air mass charged into or discharged from the air spring, instead of the air being fully charged or discharged in every cycle.

3.2.3 Result of charging process

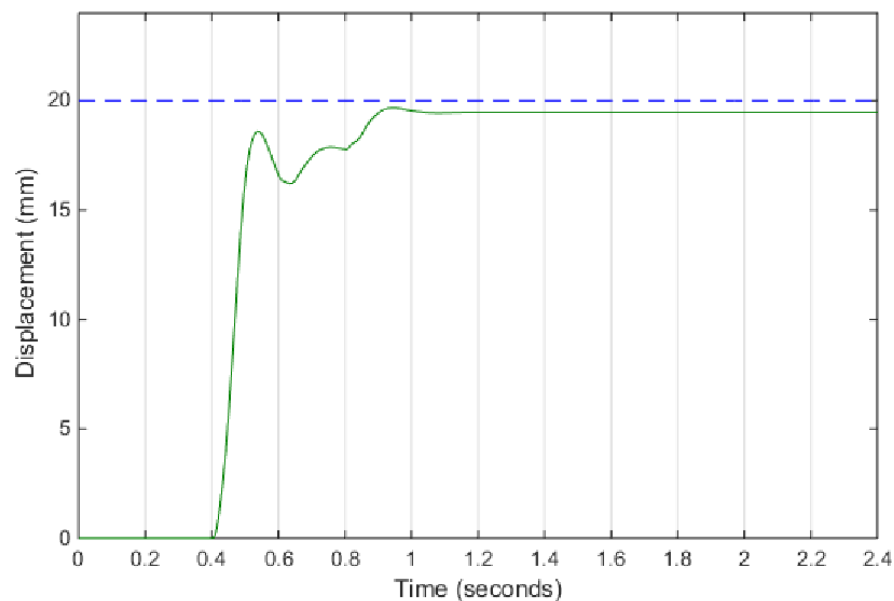


Figure 3.12 Simulation result of charging process with fuzzy controller -

displacement of the sprung mass.

In figure 3.12, the blue dotted line is the target and green line is the actual one.

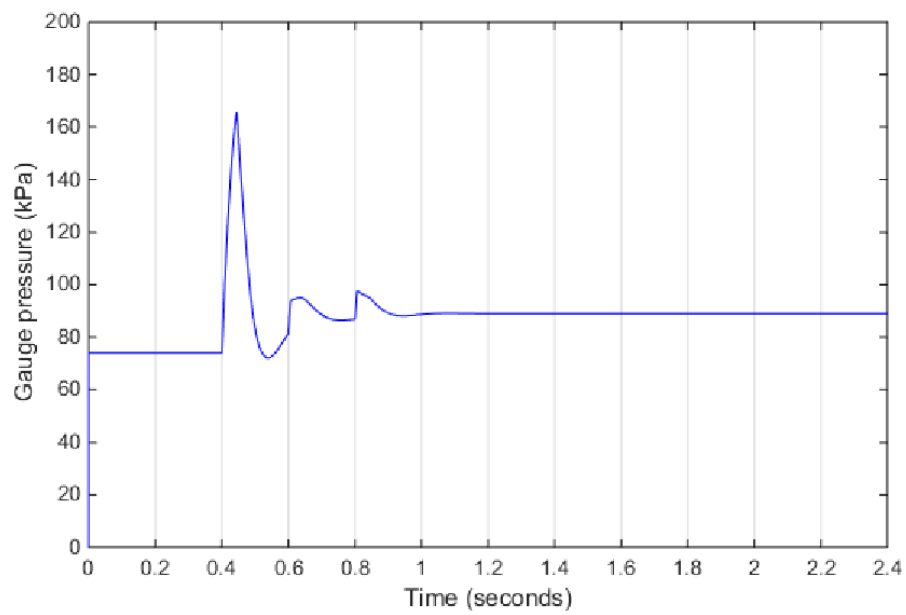


Figure 3.13 Simulation result of charging process with fuzzy controller - gauge pressure inside the air spring.

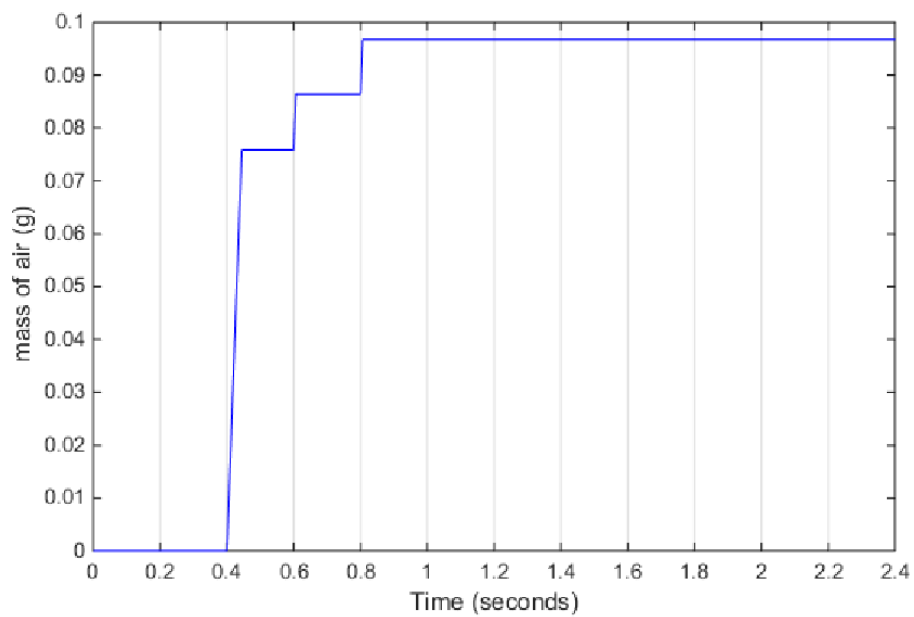


Figure 3.14 Simulation result of charging process with fuzzy controller - mass of air changed inside the air spring

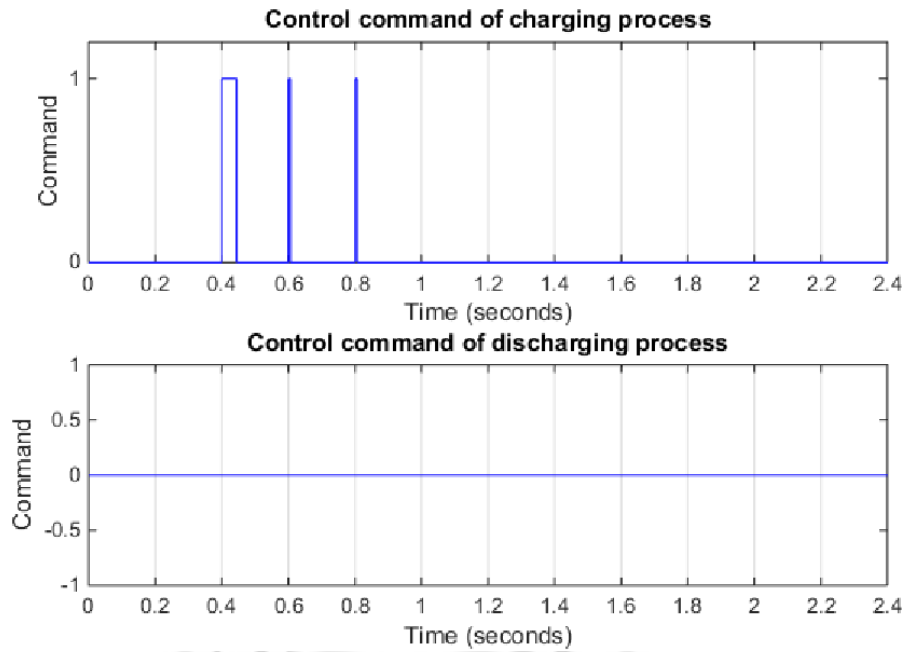


Figure 3.15 Simulation result of charging process with fuzzy controller - control

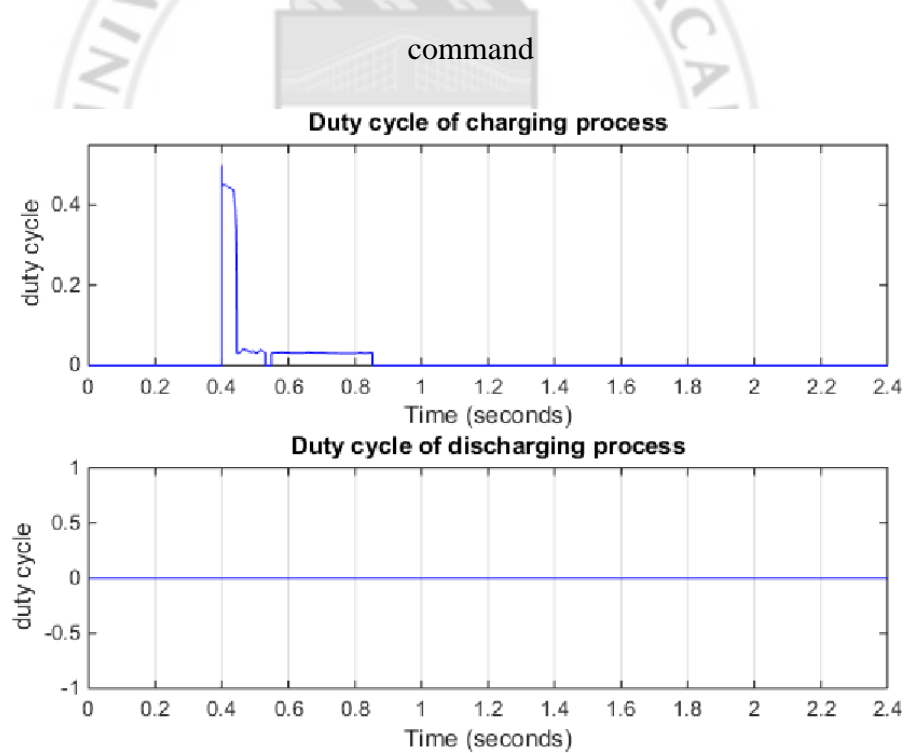


Figure 3.16 Simulation result of charging process with fuzzy controller - duty cycle

Duty cycles are the ratio of time between on and off-states of a PWM signal in a particular period. For instance, if the duty cycle is equal to 0.4 and the period is 1

second, the time of on-state in this cycle will be 0.4 second and the time of off-state will be 0.6 second. Figure 3.16 shows the estimated duty cycle which is the output of the fuzzy controller. As the period in every cycle is fixed, the duty cycles can be regarded as the opening time of the solenoid valve. After the duty cycles are estimated, they are transferred to PWM signal converter to produce PWM signal. It is the control command of the solenoid valve shown in Figure 3.15.

3.2.4 Result of discharging process

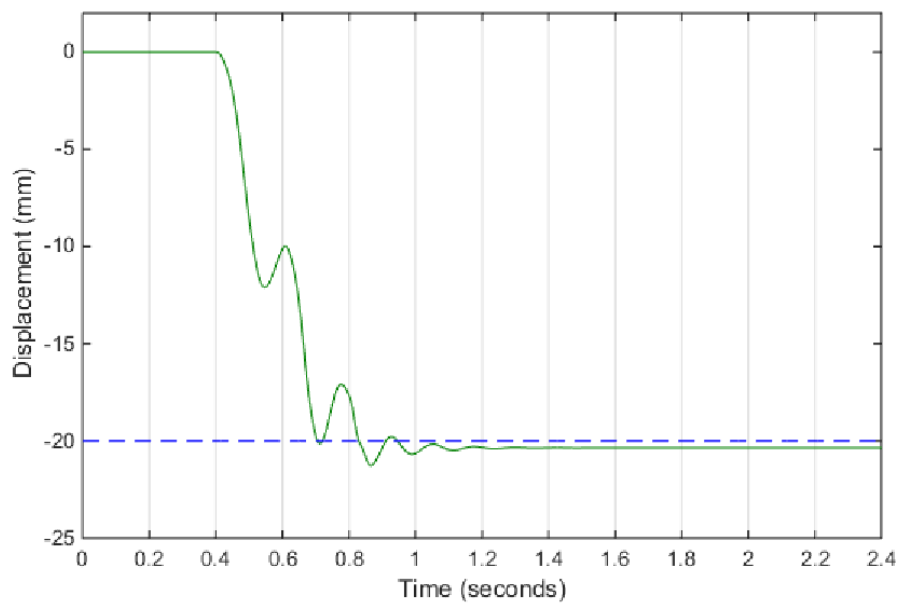


Figure 3.17 Simulation result of discharging process with fuzzy controller -
displacement of the sprung mass

In Figure 3.17, the blue dotted line is the target and green line is the actual one.

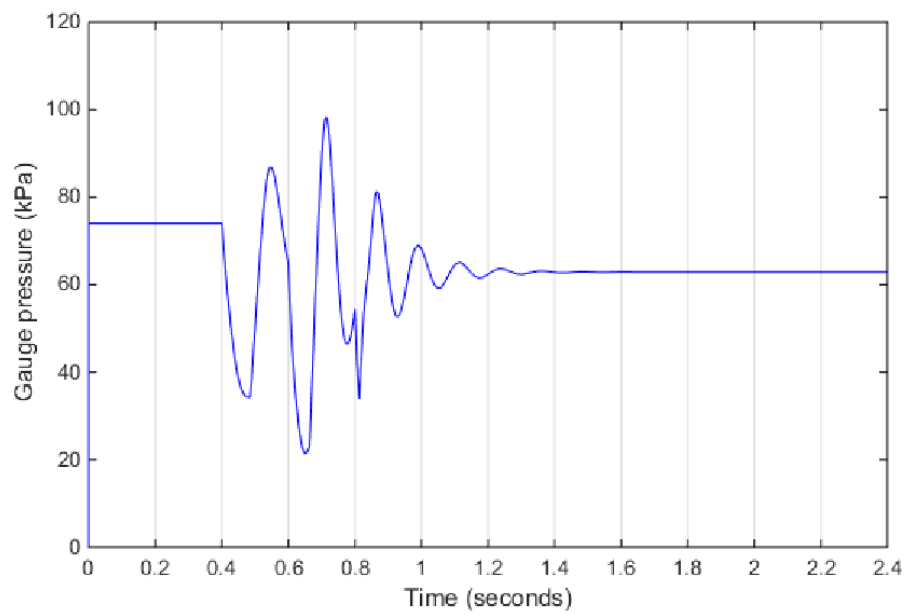


Figure 3.18 Simulation result of discharging process with fuzzy controller - gauge

pressure inside the air spring

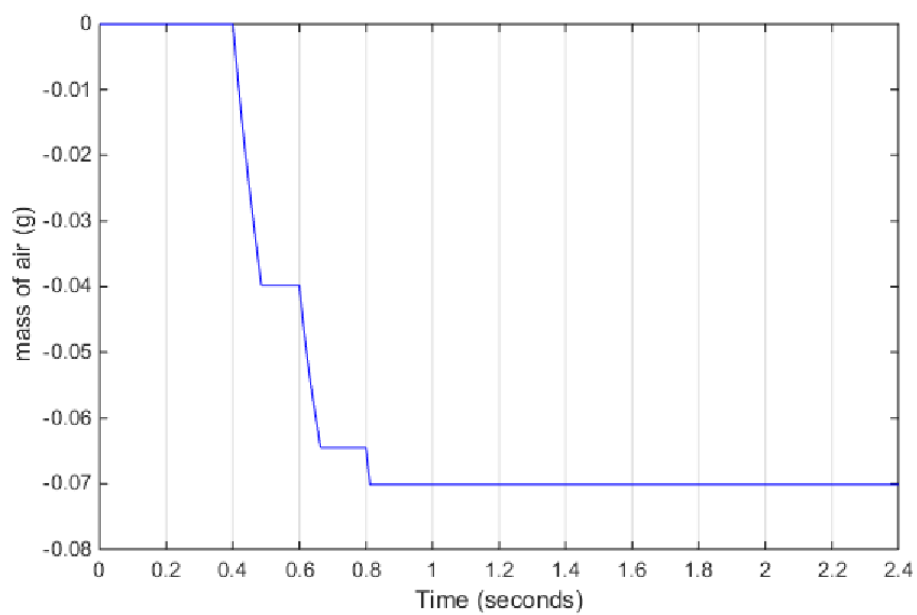


Figure 3.19 Simulation result of discharging process with fuzzy controller - mass of

air changed inside the air spring

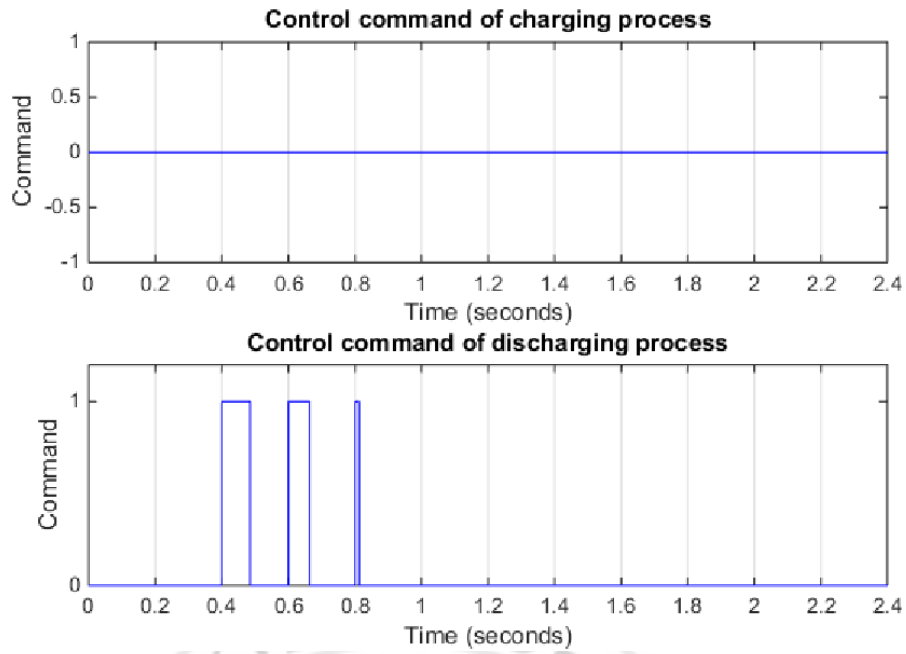


Figure 3.20 Simulation result of discharging process with fuzzy controller - control

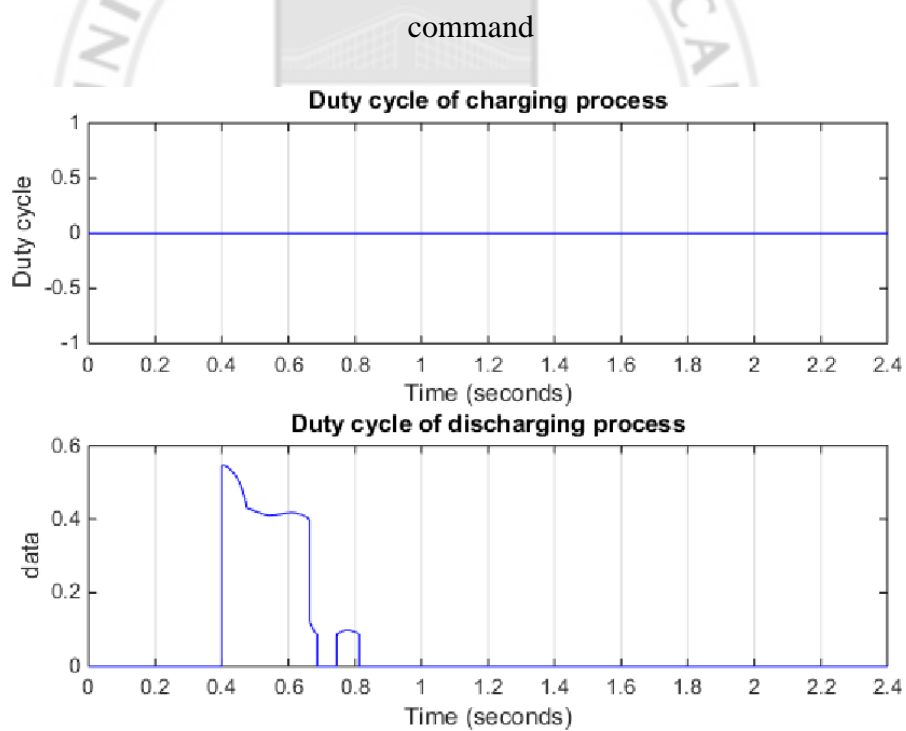


Figure 3.21 Simulation result of discharging process with fuzzy controller - duty cycle.

3.3 STATIC RIDE HEIGHT CONTROL WITH REFERENCE MODEL METHOD

3.3.1 Control concept

The core element which mainly affects the control command in the previous control strategies is the instantaneous ride height. There is a problem that the refresh rate of the processor may not catch up the rate of change of the instantaneous ride height. It will cause a result that the control command may not be transmitted to the actuator on time. In other words, the ride height may be tended to the target with several times of over-charging and over-discharging. Moreover, the control signal can directly control the amount of change of air mass. An estimation of air mass desired is effective to improve the performance in case the issue of overshooting exists frequently.

This type of control strategy is constructed on the basis of the previous strategies. A reference model is developed to estimate the air mass desired in order to approach the target. Though the control action of the ride height in the reference model approach may be done with several times of over-charging and over-discharging, only the total amount of change of air mass inside the air spring is desired. Therefore, the ride height control can be smoothly achieved.

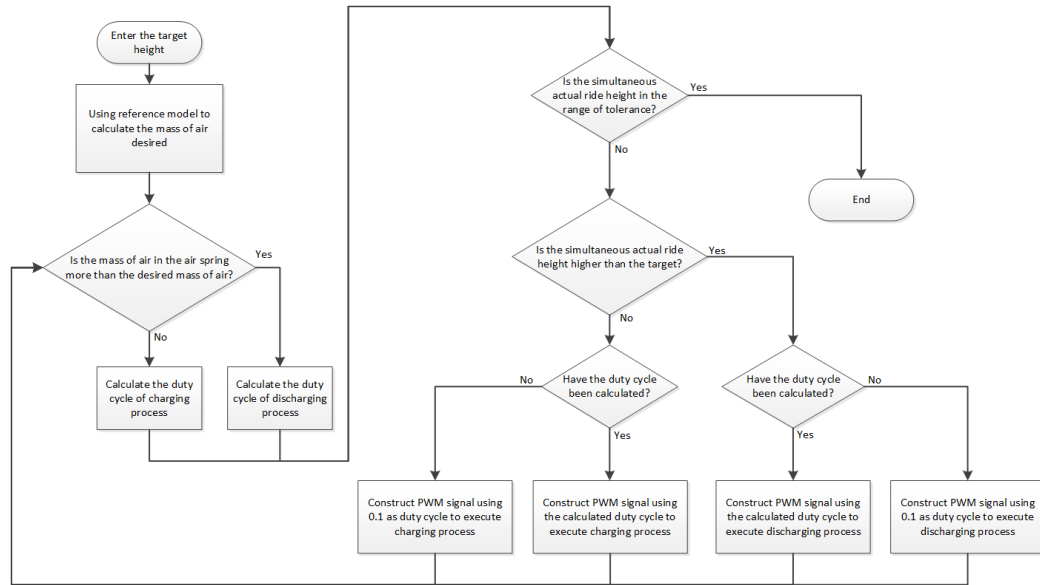


Figure 3.22 Flow chart of static ride height control with reference model

Figure 3.22 shows the logic flow of this type of control strategy. The value of target is entered into the reference model and it is turned into an amount of air mass desired. It is used in the calculation of the duty cycle of the processes. Afterwards, the system judges whether a charging or a discharging process should be executed by determining if the ride height is in the range of tolerance. It is similar to the feedback control method. Then, the selected process is executed with the calculated duty cycle.

Since the result of the reference model is just an estimation, a mismatch between the desired ride height and the desired air mass may exist. A mechanism shown at the bottom of Figure 3.22 is designed to prevent the mismatch and supplement the final output of the controller. If the process is judged to be executed but the corresponding duty cycle cannot be calculated, the smallest value of duty cycle is produced as the output. It happens when the instantaneous ride height is close to the target value.

Therefore, a micro-tuning is achieved.

3.3.2 Construction of simulation

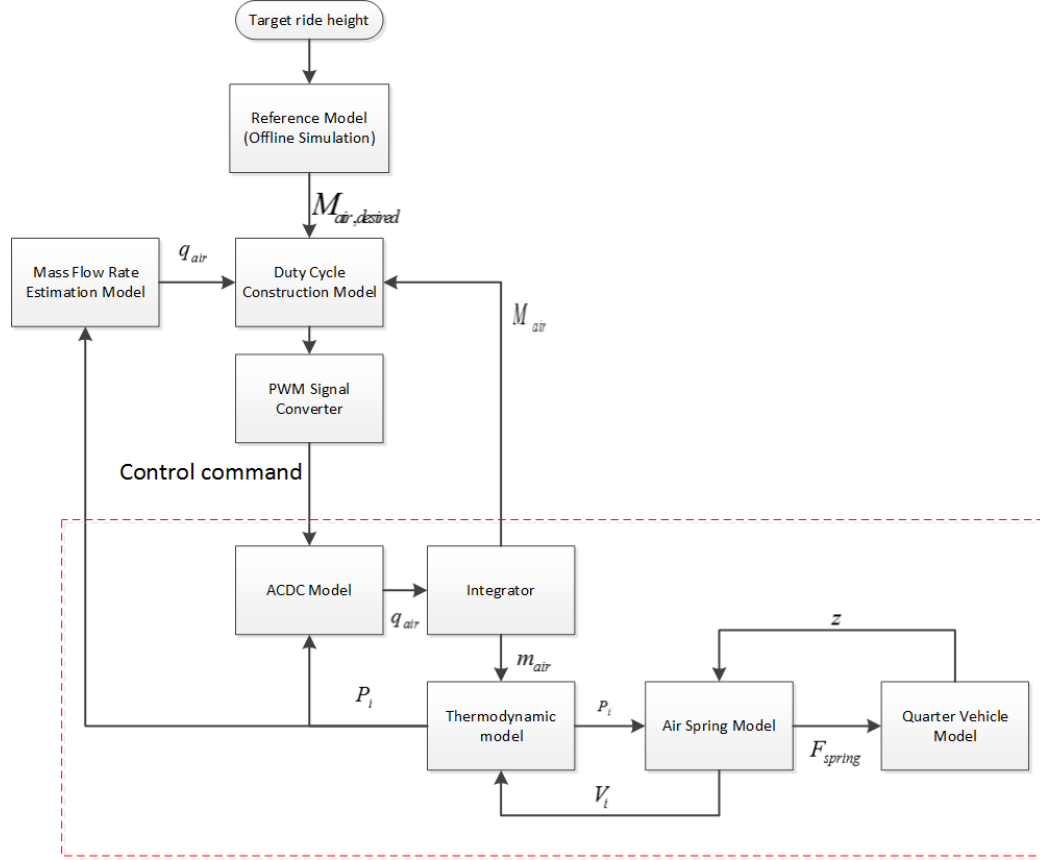


Figure 3.23 Construction of static ride height control with reference model method

Figure 3.23 shows the configuration of this control method. It is similar to the previous two methods. However, the target is entered into the controller in terms of air mass because air mass flows through the solenoid valve can be directly controlled by the opening time and the closing time of the solenoid valve. The amount of change of air mass inside the air spring can be recorded and hence the instantaneous total amount of air mass can be obtained. Afterwards, the duty cycle of charging process, $d.c.in$, and the duty cycle of discharging process, $d.c.out$, are calculated with the

equations below:

$$d.c._{in} = \frac{\Delta M_{air}}{q_{m,in}} \quad \text{when } \Delta M_{air} > 0 \quad (14)$$

$$d.c._{out} = \frac{-\Delta M_{air}}{q_{m,out}} \quad \text{when } \Delta M_{air} < 0 \quad (15)$$

$$\Delta M_{air} = M_{air,desired} - M_{air} \quad (16)$$

where $M_{air,desired}$ is the amount of air mass desired which is estimated by the reference model and M_{air} is the instantaneous total amount of air mass inside the air spring which is calculated by Eq. (7). The maximum value of duty cycle is 1 and the minimum of that is 0.

The calculated duty cycle is meant that the time needed to charge or discharge the desired amount of air mass with the instantaneous mass flow rate of air. It may be larger than 1 and it means that the time in this cycle is not enough to fulfill the target. In this case, duty cycle is set to be 1 and execute the process. Afterwards, duty cycle is calculated again in the next cycle until the ride height reaches the target.

3.3.3 Result of charging process

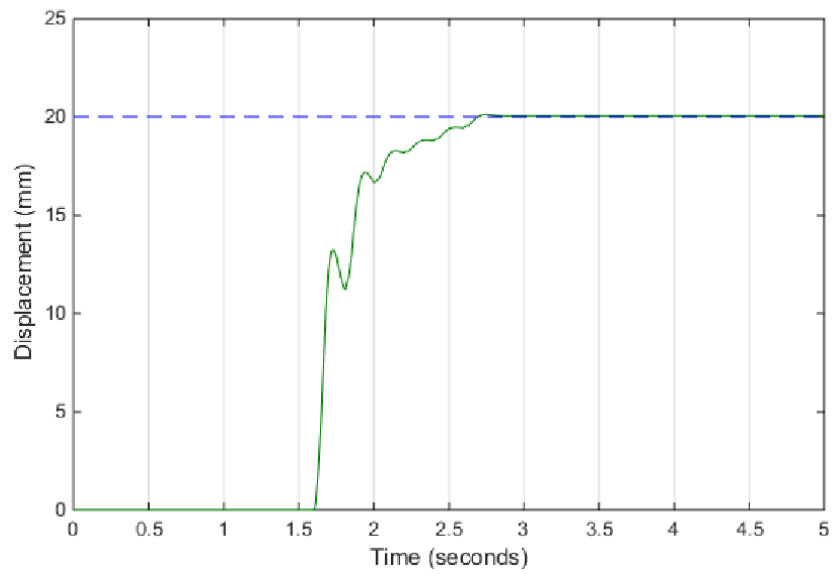


Figure 3.24 Simulation result of charging process with reference model method -

displacement of the sprung mass

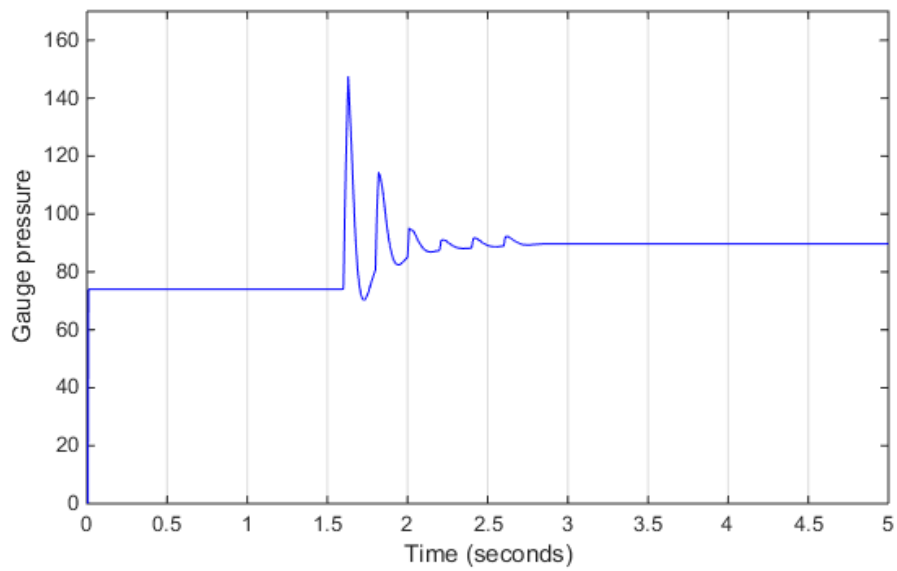


Figure 3.25 Simulation result of charging process with reference model method -

gauge pressure inside the air spring

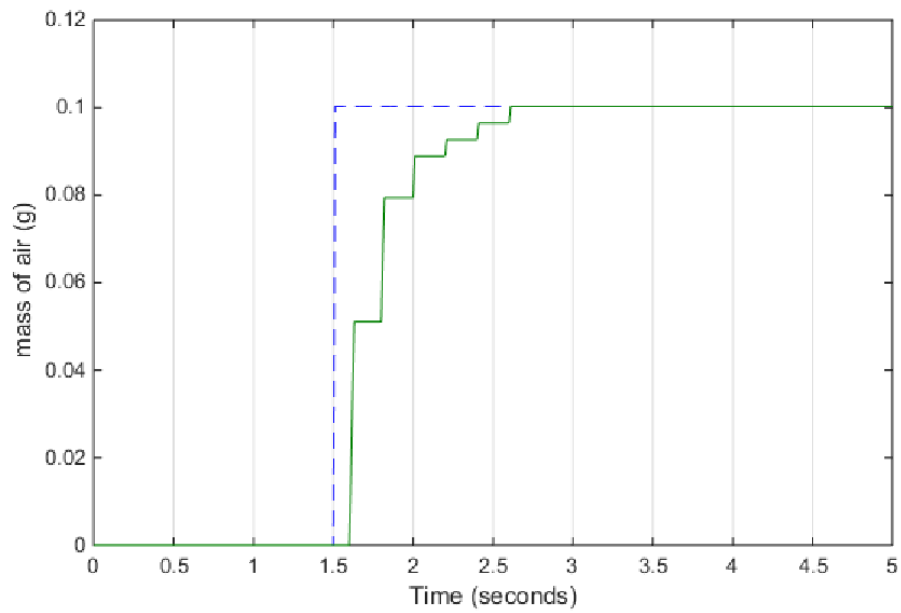


Figure 3.26 Simulation result of charging process with reference model method -

mass of air changed inside the air spring

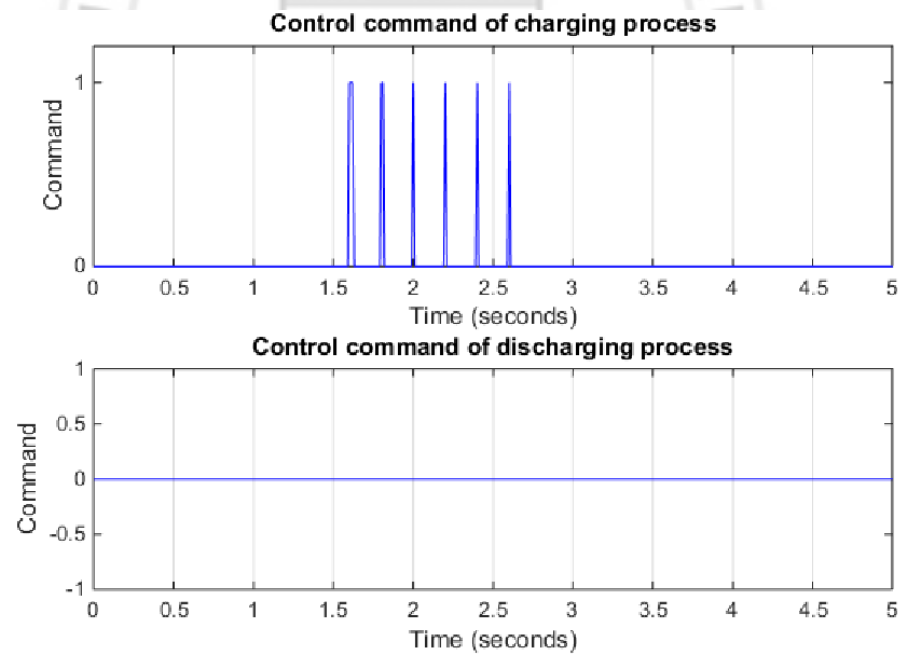


Figure 3.27 Simulation result of charging process with reference model method -

control command

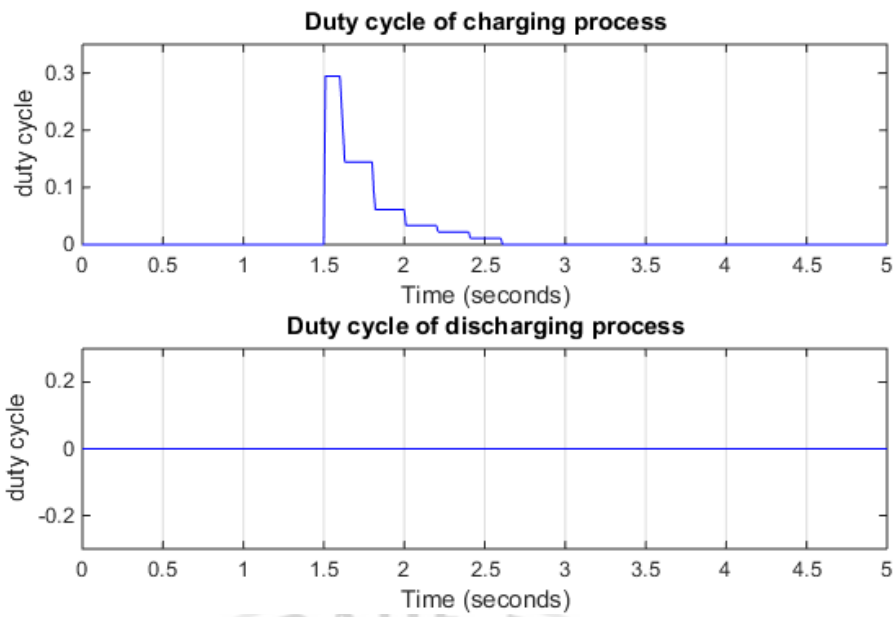


Figure 3.28 Simulation result of charging process with reference model method -

duty cycle

3.3.4 Result of discharging process

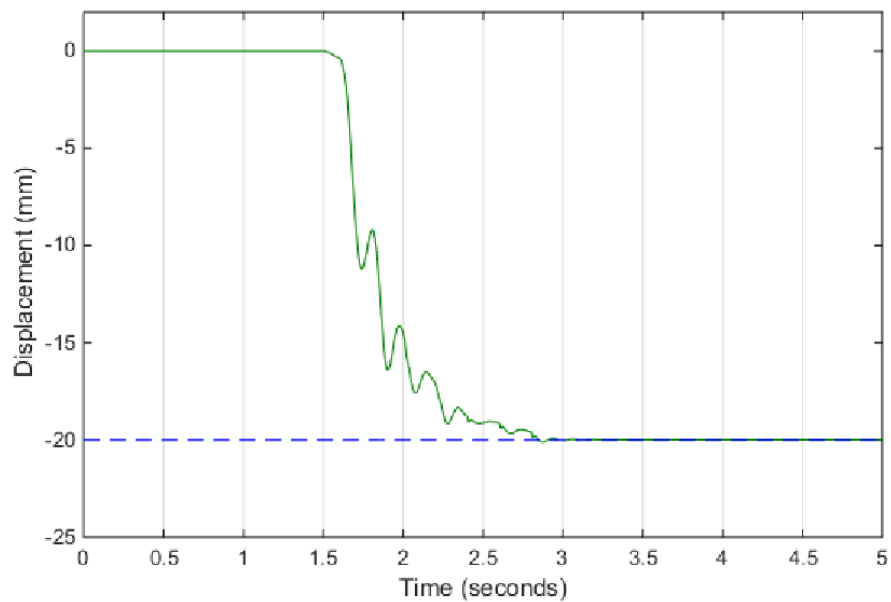


Figure 3.29 Simulation result of discharging process with reference model method -

displacement of the sprung mass

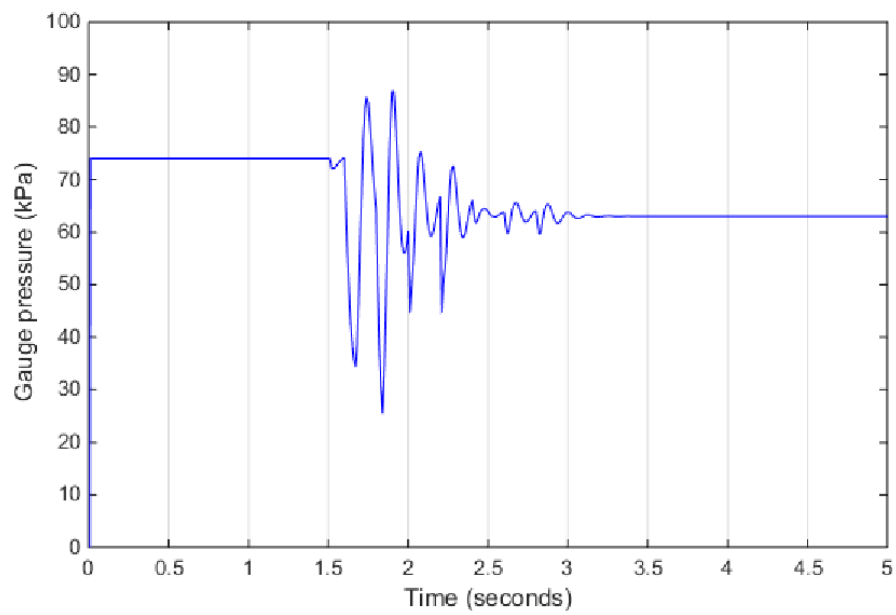


Figure 3.30 Simulation result of discharging process with reference model method -
gauge pressure inside the air spring

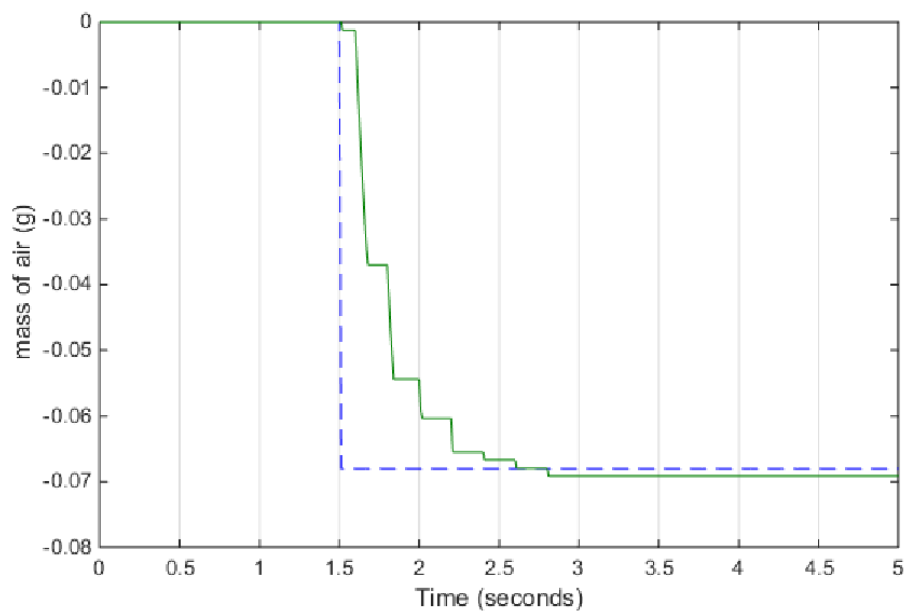


Figure 3.31 Simulation result of discharging process with reference model method -
mass of air changed inside the air spring

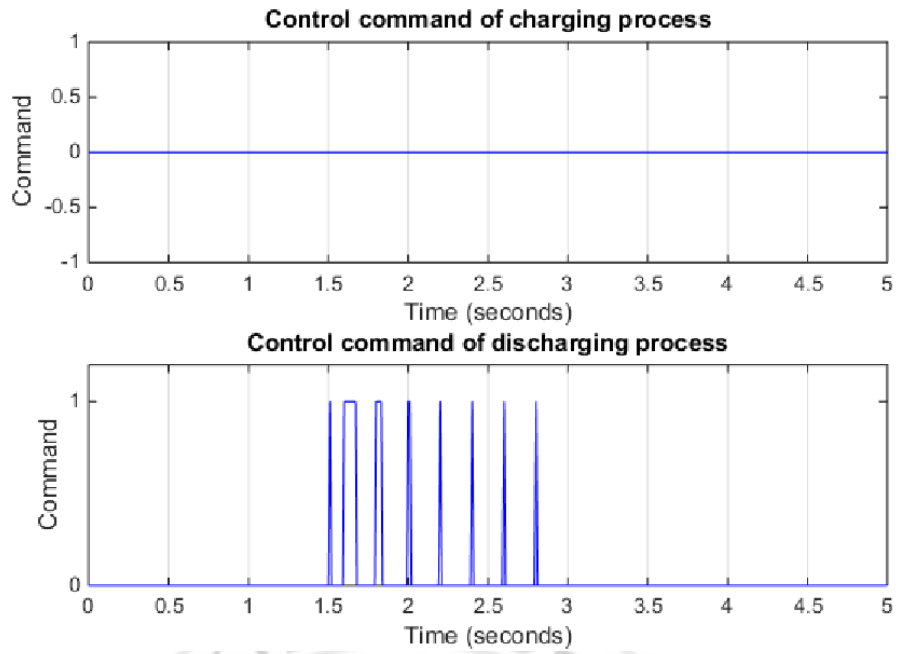


Figure 3.32 Simulation result of discharging process with reference model method -

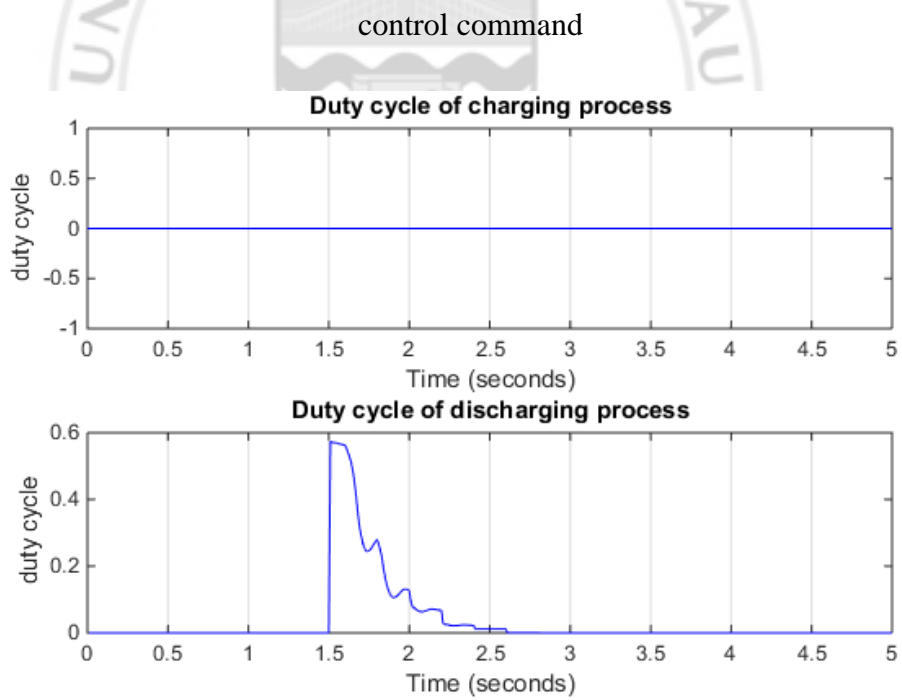


Figure 3.33 Simulation result of discharging process with reference model method –

duty cycle

3.4 DISCUSSION OF SIMULATION RESULTS

Figures 3.3 to 3.6 show the simulation results of charging process controlled with feedback control method. By comparing Figures 3.3 and 3.4, the displacement of the sprung mass is not directly related to the pressure inside the air spring. The pressure is increased while the ride height is raised. However, the pressure drops down and even over the original level when the displacement of the sprung mass tends to stop. It is claimed that the pressure does not directly affect the ride height but it is a kind of force exerted to the sprung mass. The pressure remains stable as the ride height reaches the target and stops the process. It is different from the original level though the load is not increased because the supporting force of the sprung mass is shared by the damper and the air spring with an unknown ratio. The result of different amount of pressure is claimed as the portion of the air spring is changed when the ride height is changed. Additionally, the pressure is changed rapidly when the air spring is needed to be inflated and deflated repeatedly. It can be observed in Figure 3.8.

It is clear from the comparison between Figures 3.4 and 3.5 that the pressure inside the air spring is partially affected by the change of air mass inside the air spring. The pressure is increased as the air mass is being charged into the air spring and vice versa. However, the pressure is slightly increased when the solenoid valve are just

closed and the mass of air is stopped flowing through the solenoid valve due to the compressibility of air.

In Figures 3.5 and 3.6, the relationship between the solenoid valve and the mass of air changed inside the air spring is shown. It is obvious that the change of mass of air can be controlled by controlling the opening time and the closing time of the solenoid valve.

By comparing Figures 3.15, 3.16, 3.20 and 3.21, the fuzzy controller is verified that it can be worked to estimate a suitable duty cycle to execute the process. The result of the ride height shown in Figures 3.12 and 3.17 indicate that the fuzzy controller is better than the result of feedback control method shown in Figures 3.3 and 3.7. The correction of surplus air mass is eliminated. Moreover, Figures 3.6, 3.10, 3.15 and 3.20 reveal that the frequencies of charging and discharging processes are also reduced.

In Figures 3.26 and 3.31, the change of air mass was caught up the mass of air desired which is estimated by the reference model. Accurate performance is obtained as shown in Figures 3.24 and 3.29. Figures 3.28 and 3.33 show that the processes are executed smoothly. The duty cycles are decreased smoothly rather than changed sharply. Therefore, it is claimed that the reference model method can provide good adjustment.

Overall, the simulation results can be summarized in Tables 3.2 and 3.3.

Table 3.3 Summary of simulation results of charging processes

	Feedback control method	Fuzzy controller	Reference model
Time taken (s)	0.54	0.4	1
Error (mm)	0.85	0.54	-0.06
Max.% of overshoot	40%	0	0

Table 3.4 Summary of simulation results of discharging processes

	Feedback control method	Fuzzy controller	Reference model
Time taken (s)	0.48	0.41	1.3
Error (mm)	0.8	0.35	-0.01
Max.% of overshoot	32%	0	0

As a short conclusion of simulation results, the feedback control method cannot perform very well. It needs several times of over-charging and over-discharging processes before stable.

The fuzzy controller provides the fastest adjustment speed with an acceptable error. The over-charging and over-discharging are not found. It means that the adjustment is finished in a smooth way instead of hunting.

The reference model method takes the longest time to adjust the ride height. However, it provides the most accurate results among the three methods. The over-charging and over-discharging processes are not found.

By comparing the simulation results, the fuzzy controller provides the best performance in terms of precision and adjustment speed. Though the reference model method provides a more accurate result, the time taken is twice or even three times more than the fuzzy controller. By considering the compromise between accuracy and adjustment speed, the fuzzy controller is selected to implement on the RHC system.



CHAPTER 4: IMPLEMENTATION OF THE RIDE HEIGHT CONTROL SYSTEM

In this chapter, the details of the experimental implementation of the designed RHC system for a quarter car with air suspension are presented. The RHC system is separated into two parts: air tank system and the ACDC system.

Moreover, a brief introduction of signal processing devices and software used are presented in this chapter. Additionally, the construction of a QCTR with air suspension is introduced.

4.1 CONSTRUCTION OF THE RIDE HEIGHT CONTROL SYSTEM

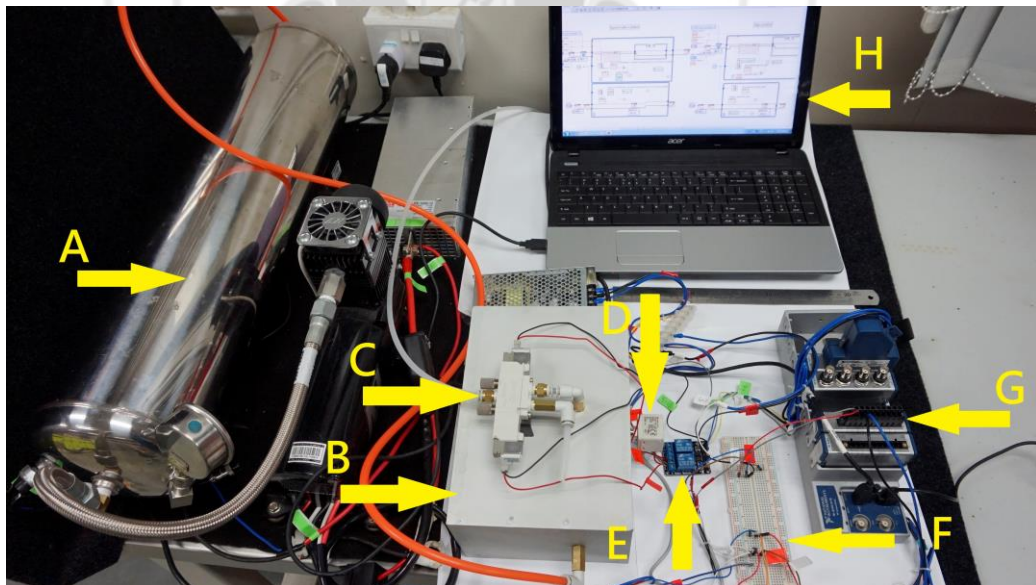


Figure 4.1 Overview of ride height control system.

Figure 4.1 shows the overview of the RHC system. The components of RHC system are listed as following:

- A. An air compressor connected with air tank;
- B. A customized air reservoir;
- C. Solenoid valve;
- D. An air pressure sensor;
- E. Two electromagnetic relays;
- F. A solderless-breadboard with circuits;
- G. The NI-DAQ modules with the NI-cDAQ;
- H. The interface of the LabVIEW 2014.

The software in the ACDC system are the NI MAX, LabVIEW 2014, VeriStand 2014 and MATLAB 2014.

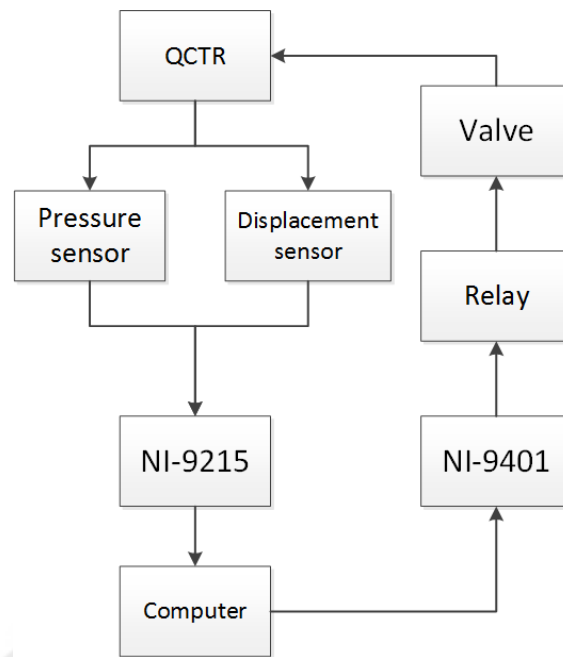


Figure 4.2 Block diagram of interconnection among the QCTR, RHC system and control and data acquisition hardware

Figure 4.2 illustrates the interconnection among the QCTR, RHC system, and control and data acquisition hardware. First, displacement sensor and air pressure sensor receive the instantaneous signals from QCTR and transmitted to NI-9215 and computer for processing.

After processing, series of PWM signals transmitted to NI-9401 and produce digital control signals. The signals transmit to the electric relays to change the states of the solenoid valve for charging or discharging the air spring in order to adjust the ride height. Then the sensors receive the instantaneous signals after the latest adjustment and repeat the cycle mentioned before.

4.1.1 Air tank system

The air tank system contains one air compressor, one 5 gallons air tank, one customized air reservoir and the connecting tubes.

First, the air compressor draws the air from the surrounding atmosphere, compresses the air and delivers into the air tank. Secondly, the compressed air is delivered into the air reservoir and stored for the requests from the ACDC process.

Finally the air reservoir delivers the air to the air spring via solenoid valve. Table 4.1 shows the specification of air compressor.

Table 4.1 Specification of air compressor

Air compressor by AIR-ZENITH	
Working Voltage	12V DC
Working Pressure	200 psi (about 1379 kPa)
Air Flow	4.25 cfm (about 0.002005 m^3/s)
Motor	$\frac{3}{4}$ Horse Power

4.1.2 Air charging and discharging system

The ACDC system includes solenoid valve, two electromagnetic relays, a circuit, NI-cDAQ chassis with two NI-DAQ modules. The solenoid valve are used to charge the air into the air spring or discharge the air from the air spring.

There are three states and ports connections shown in Figure 4.3: port 1 and port 3 are sealed; port 2 is connected to air spring; port 4 is connected to air reservoir; port 5 is connected to the atmosphere.

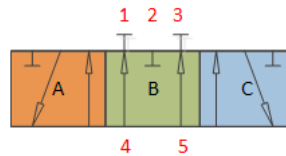


Figure 4.3 Illustration of solenoid valve

Normally, the valve stays at state B as there is no any process required. If the charging process is executed, the valve turns into state A and the air spring will be connected to the air reservoir.

Otherwise, if the discharging process is executed, the valve turns into state C and the air spring will be connected to the atmosphere.

Furthermore there are three displacement sensors and one air pressure sensor mounted on QCTR to receive the analog signals.

Table 4.2 to Table 4.4 shows the specification of the solenoid valve and the sensors.

Table 4.2 Specification of the solenoid valve

Solenoid valve by SMC	
Fluid	Air
Internal pilot operating pressure range	0.2 MPa to 0.7 MPa
Maximum operating frequency	3 Hz

Table 4.3 Specification of displacement sensor

Displacement sensor by Shanghai Tianmu	
Displacement range	0 mm to 1000 mm
Resolution	0.03 mm
Current Output	4 mA to 20 mA

Table 4.4 Specification of air pressure sensor

Air pressure sensor by SMC	
Rated pressure range	-0.1 MPa to 1.0 MPa
Repeat accuracy	$\pm 0.2\%$ F.S. ± 1 digit
Voltage output	1 V to 5 V ($\pm 2.5\%$ F.S.)

4.2 SIGNAL PROCESSING DEVICES AND SOFTWARE

To implement the proposed RHC system on a QCTR with air suspension, three National Instrument™ devices are used in the experiments; they are NI-9215, NI-9401 and NI cDAQ-9178.

NI-9215 module is used for collecting the analog signal, NI-9401 module is used for emitting digital signal and NI cDAQ-9178 chassis is used as a transmitter for the analog signals from the NI-9215 to computer and digital signals emitted from computer to NI-9401.

The VeriStand 2014 is a graphical programming platform for the user to control the NI devices. These devices serve as the interface between signals from the QCTR and the computer. It also helps users to control the NI instruments. In addition, MATLAB plug-in is available in VeriStand, so the MATLAB script can be embedded into VeriStand directly as a support to the users.

4.2.1 Data acquisition and processing

The displacement sensors collect the instantaneous displacements of three different positions on the test rig respectively. They are the road surface, the sprung part of the suspension and the unsprung part of the suspension. Then each of the displacement sensors produces a related current for the related displacements of each position to the NI-9215 respectively. The locations of the three displacement sensors are shown in Figure 4.6.

The air pressure sensor also collects the internal air pressure of air bag of the air spring and produces a related voltage to the NI-9215. Then all the analog signals transited by the NI-9215 to the chassis NI cDAQ-9178 are delivered to the computer for the calculation and storing.

Table 4.5 to Table 4.7 shows the specification of the NI equipment which are used in the experiment.

Table 4.5 Specifications of NI module: NI 9215

NI 9215	
Type	Simultaneous analog input
Channels	4 differential
Signal range	± 10 V
Sample rate	100 kS/s/ch
Resolution	16-Bit

Table 4.6 Specifications of NI module: NI 9401

NI 9401	
Type	Digital input/output
Channels	8 Digital input/output
Signal levels	5 V/TTL
Signal switching frequency(2 output channels)	20 MHz/ch
Direction	Bidirectional

Table 4.7 Specifications of NI chassis: cDAQ-9178

NI cDAQ-9178	
Slots	8
Counters	4
Number of simultaneous tasks	7
Number of AI timing engines	3
BNC triggers connections	Up to 1 MHz clocks and triggers

4.2.2 Control software

After the analog signals are delivered into computer, VeriStand starts to process the signals to achieve the ride height control purpose.

First, the signals pass through a low-pass filter to be filter out the noise. After signal conversion, the signals can be displayed in meter representing the actual height of the sprung part and the unsprung parts; the internal pressure of the air bag of the air spring suspension system can also be displayed from the original voltage to the Pascale on the working space of the VeriStand 2014.

Then the data are analyzed by the MATLAB plug-in on VeriStand. The corresponding PWM signal is produced and transmitted to the NI cDAQ-9178 chassis. Afterwards, NI-9401 outputs the control signal which controls the electric relays to change the states of the solenoid valve, thus the ACDC process can be executed.

4.3 AIR SUSPENSION SYSTEM AND QUARTER CAR TEST RIG

In the QCTR, the ride height control is provided by the response of the air bag by the air volume change. The displacement sensors are connected to the test rig for collecting the instantaneous data to control of the ride height.

In the following section, the inflatable air spring system, the suspension system and the quarter car test rig are introduced respectively.



Figure 4.4 Overview of the quarter car test rig with sensors

In Figure 4.4 shows the connection of QCTR and sensors. The components of QCTR are listed as following:

- A. Air spring;
- B. Damper;
- C. Damper controller.

4.3.1 Inflatable air spring system

The air spring provides a quick response in the change of height of the suspension part in the QCTR, which depends on the internal volume change of the air bag. The air suspension system is shown in the part A of Figure 4.4.

The damper connected in parallel with the air spring provides damping force for the suspension system. In this test rig, the damper also has an independent controller to turn the strength of the damper. The damper is shown in the part B and the damping controller is shown in the part C in the Figure 4.4.

The inflatable air spring system provides a comfortable riding quality, variable stiffness and ride height of the suspension system. With a suspension system with inflatable air spring, the vehicles can try to keep chassis at the same level under various loading, roads and driving conditions.

4.3.2 Quarter car test rig

This QCTR is used to implement the RHC system designed in the previous section. This test rig is designed based on the suspension system of the Honda Civic EG-series with the double wishbone suspension system, but it is replaced the original coil spring with an inflatable air spring.

Apart from that, this test rig can be added extra loadings at the back of it, for making this test rig more similar to the weight of an actual quarter car. The position of the back of the test rig for adding the loads is shown in Figure 4.5.

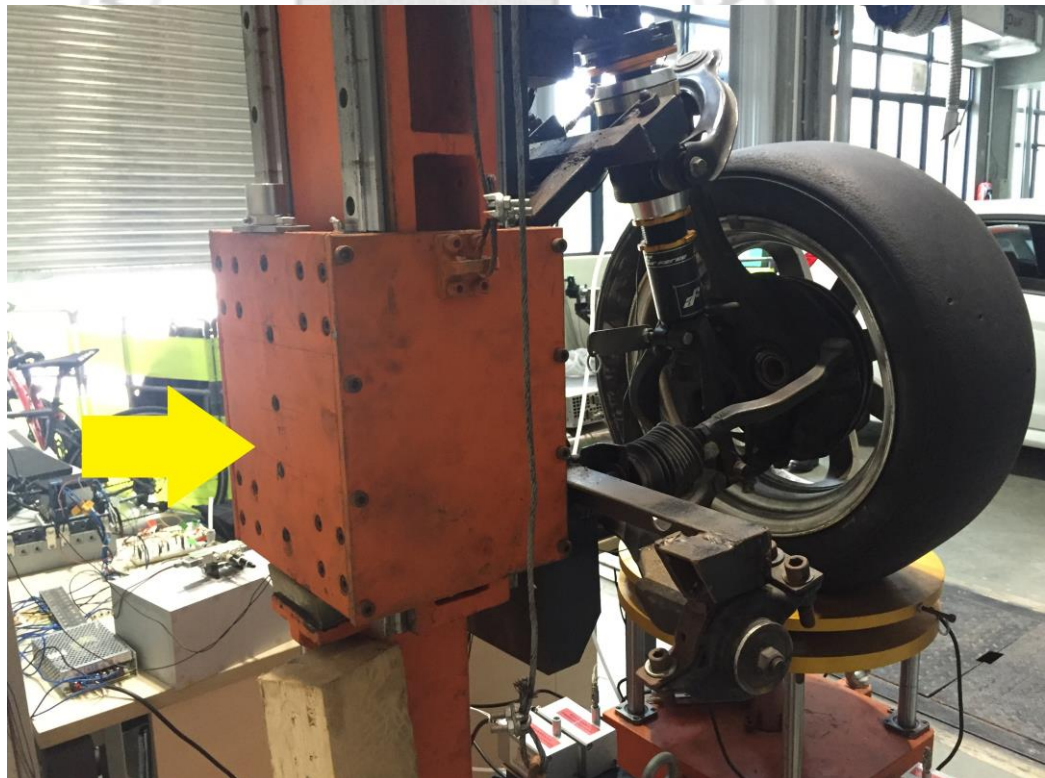


Figure 4.5 Rear view of the QCTR

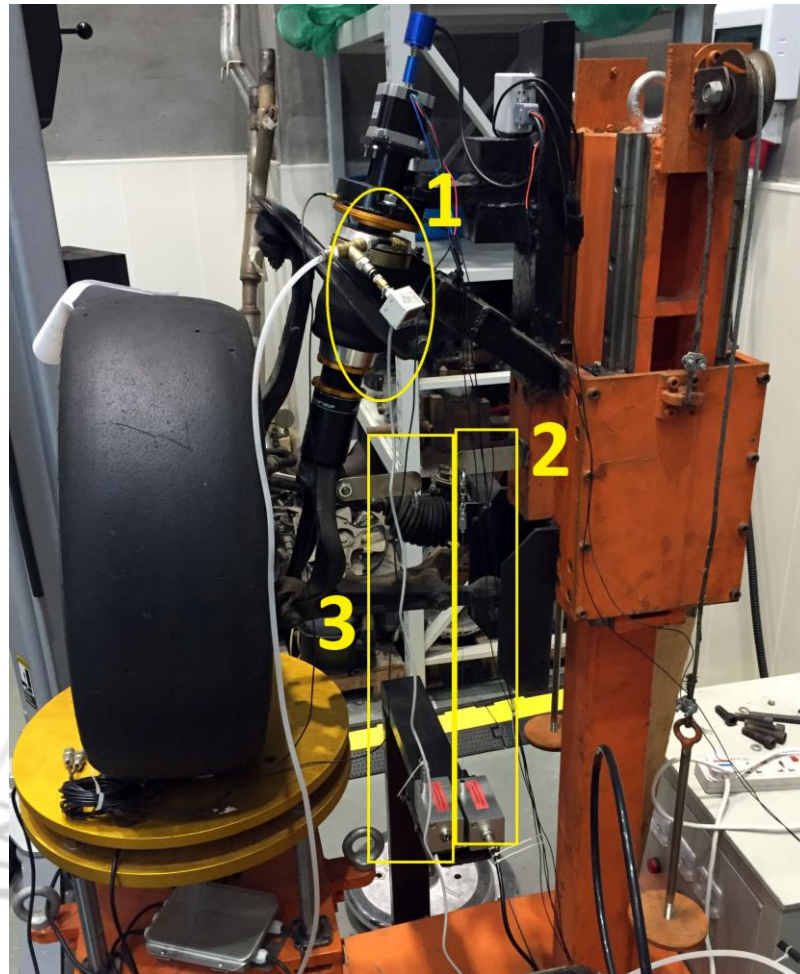


Figure 4.6 Positions of the sensors and the structure of the suspension system

In Figure 4.6 shows the corresponding positions of the sensors:

1. The air pressure sensor;
2. The displacement sensor of the sprung part;
3. The displacement of the sprung part.

Besides, the structure of the double wishbone is also shown in Figure 4.6.

CHAPTER 5: EXPERIMENTAL RESULTS

The fuzzy controller is implemented on the RHC system and a series of experimental results are shown in this chapter. It verifies the functionality of the RHC system.

5.1 STATIC RIDE HEIGHT CONTROL WITH FUZZY CONTROLLER

5.1.1 Result of charging process

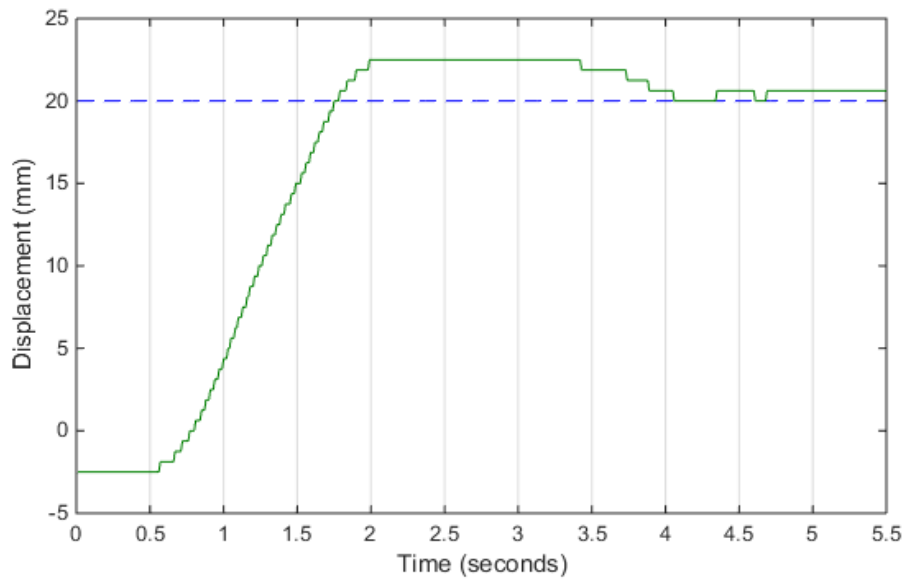


Figure 5.1 Experimental result of charging process with fuzzy controller -

displacement of the sprung mass

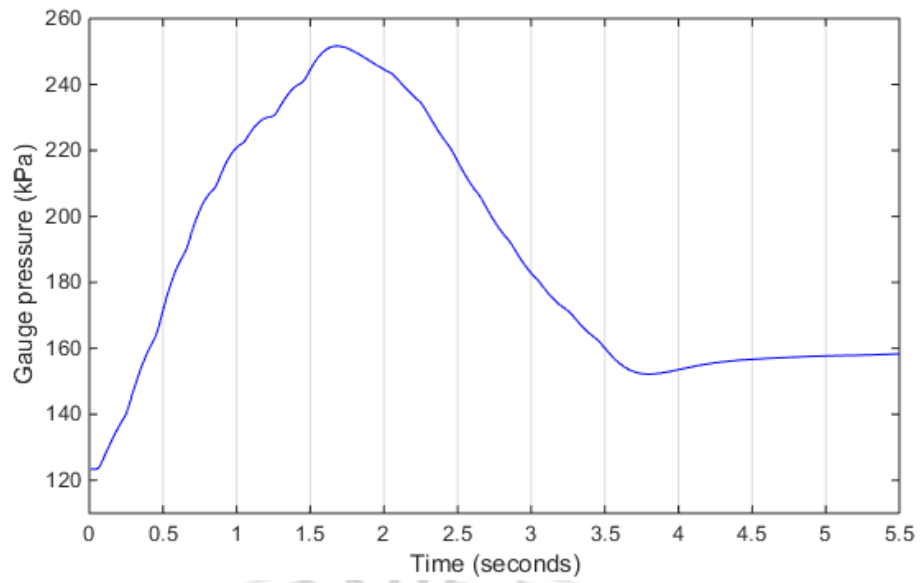


Figure 5.2 Experimental result of charging process with fuzzy controller - gauge pressure inside the air spring

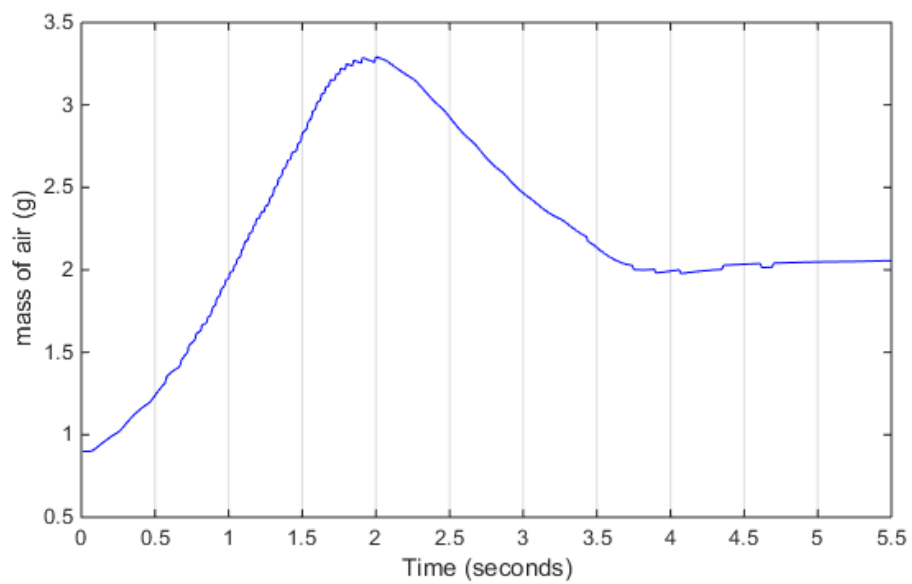


Figure 5.3 Experimental result of charging process with fuzzy controller – amount of mass of air inside the air spring

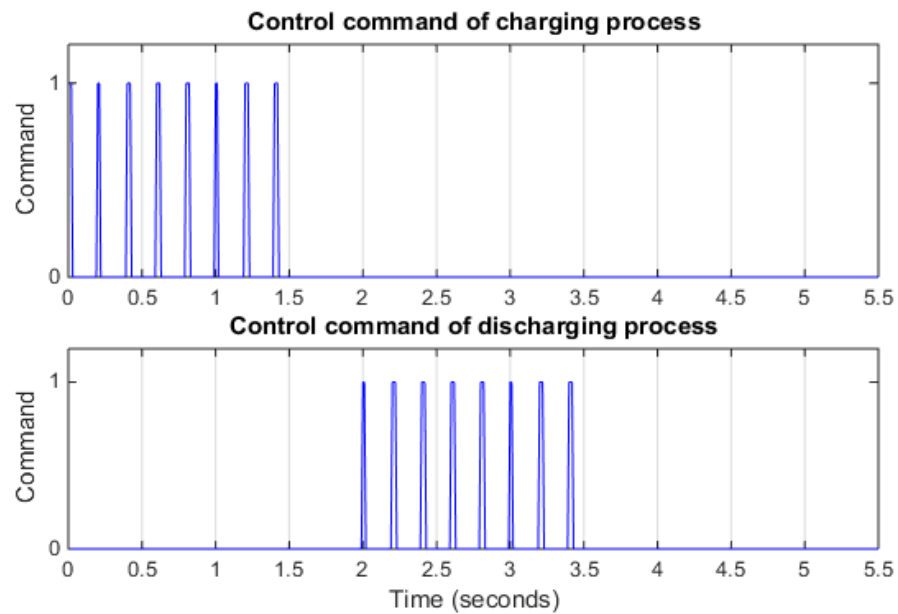


Figure 5.4 Experimental result of charging process with fuzzy controller - control command

By comparing the experimental results with the simulation results which are shown in Figures 3.12 to 3.16, the error is slightly larger than that in the simulation. The ride height is slightly over the target. There is an extra discharging process executed in the test. The trend of the pressure inside the air spring is also different due to the uncertainty of the properties of air.

5.1.2 Result of discharging process

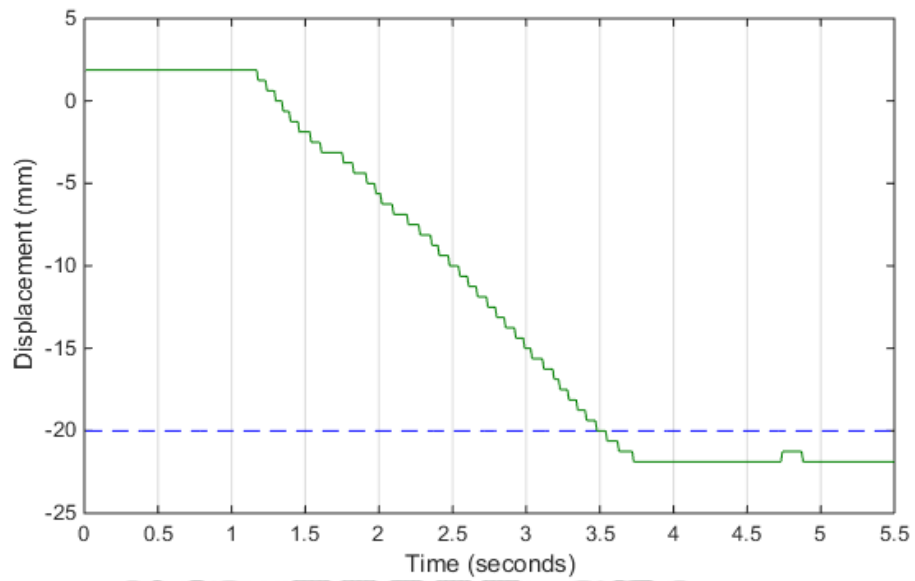


Figure 5.5 Experimental result of discharging process with fuzzy controller -

displacement of the sprung mass

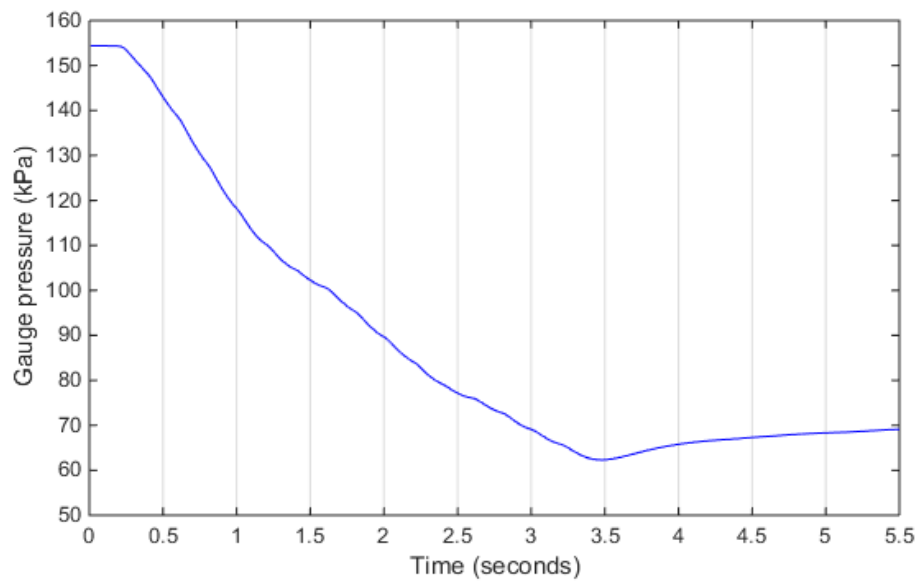


Figure 5.6 Experimental result of discharging process with fuzzy controller - gauge

pressure inside the air spring

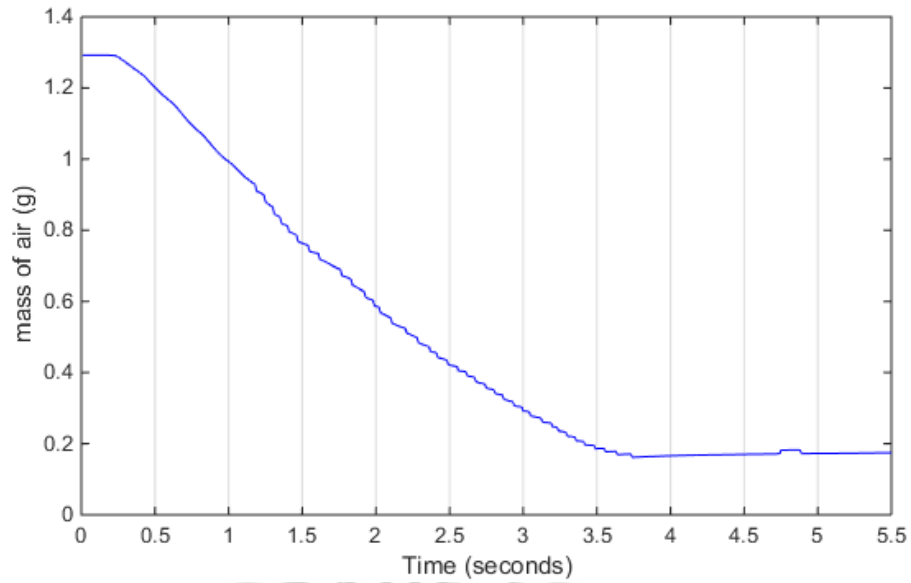


Figure 5.7 Experimental result of discharging process with fuzzy controller –

amount of mass of air inside the air spring

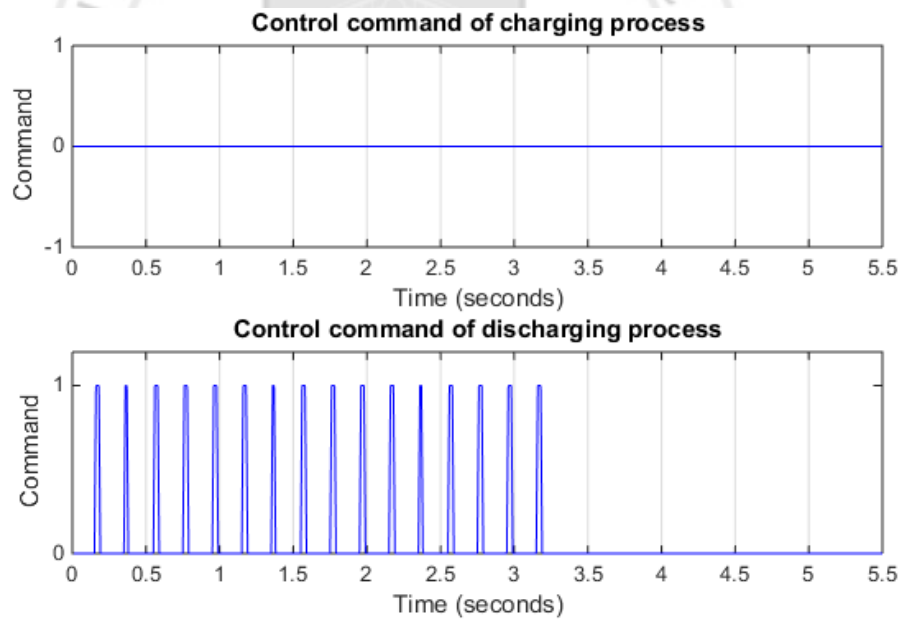


Figure 5.8 Experimental result of discharging process with fuzzy controller - control

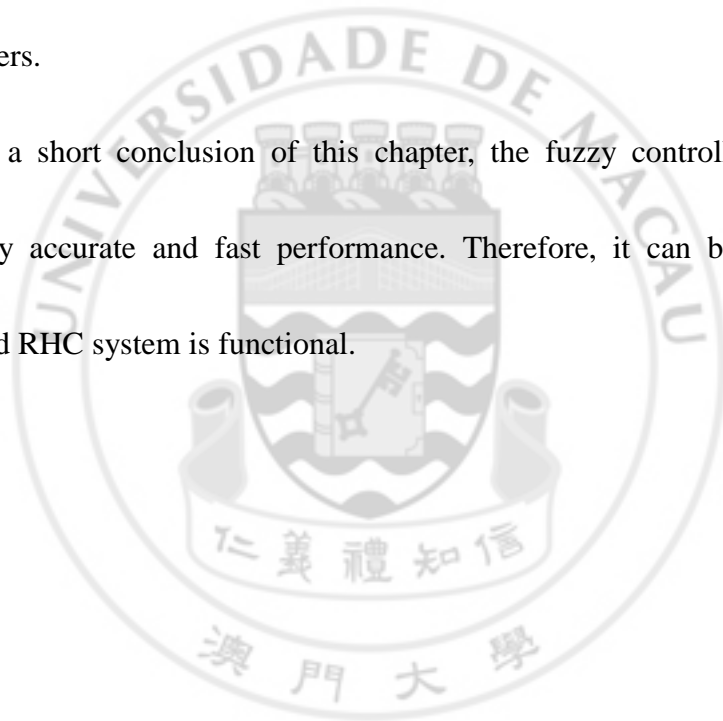
command

Figures 5.13 to 5.16 show the experimental result of discharging process with the fuzzy controller.

5.2 DISCUSSION OF EXPERIMENTAL RESULTS

By comparing with the simulation results, the RHC system in experiment takes more time to complete the adjustment. An over-charging action occurs in the experiment of charging process. There are some possible reasons: The controller actual performance is slightly worse than the simulation result the problem may come from the noise of the sensors and the difference between the simulation and test rig parameters.

As a short conclusion of this chapter, the fuzzy controller still provides a relatively accurate and fast performance. Therefore, it can be claimed that the proposed RHC system is functional.



CHAPTER 6: CONCLUSIONS

6.1 SUMMARY

Firstly, a nonlinear mathematical model of a quarter car with active air suspension system is developed. The air charging and discharging model was also involved. It can be used to shorten the time taken in the design of control strategy. In addition, it can also be a type of reference model to predict the state of the system.

Secondly, by comparing the simulation results of different kinds of control strategies, fuzzy controller was selected by analyzing a series of simulation results and experimental results. It performed well in the perspective of accuracy and the speed of adjustment. Fuzzy control strategy was finally chosen to implement in the RHC system.

Thirdly, the RHC system was designed and implemented to the QCTR. The experiments were set up in which NI devices, LabVIEW, VeriStand and MATLAB were utilized. The pneumatic circuit and the electronic control circuit were constructed and connected to the QCTR. The signal of the QCTR and ACDC system were studied and analyzed and the RHC system was proved by the experiments that it could be functional.

6.2 ORIGINALITIES

The originalities of this project include:

- 1) A nonlinear mathematical model, which consists of a quarter car model with an active air suspension system and an air charging and discharging model, is developed on the basis of vehicle dynamics and thermodynamics;
- 2) A RHC system is designed and implemented on a QCTR. A pneumatic circuit and the corresponding electronic control circuit are designed;
- 3) A new control strategy of reference model method based on air mass is developed;
- 4) Comparisons among feedback control method, fuzzy controller and reference model method for ride height control is an original work.

6.3 RECOMMENDATION FOR FUTURE WORK

This work is a preliminary study only, so the following future work is suggested:

- (1) Various controllers, such as sliding mode control (SMC), proportional-Integral-Derivative (PID) control, model predictive control (MPC) and linear-quadratic regulator (LQR) control, can be implemented for RHC system for comparison.

- (2) Reference model method can be combined with other control algorithms to obtain a faster, more stable and more accurate performance.
- (3) The limitations in hardware implementation, such as the time delay problem and the signal noise problem, will be analyzed and hopefully be improved in the following work.
- (4) A dynamic RHC system can be studied to strengthen the application of the ride height adjustment.



REFERENCE

- [1] Y. Chen, J. He, M. King, W. Chen, and W. Zhang, "Effect of driving conditions and suspension parameters on dynamic load-sharing of longitudinal-connected air suspensions," *Science China Technological Sciences*, vol. 56, pp. 666-676, 2013.
- [2] K. Ogawa, K. Satoh, and T. Enomoto, "Development of damping control system for air suspension," *JSAE Review*, vol. 17, pp. 322-324, 7// 1996.
- [3] H. Kim, Y. Kim, and D. Shin, "Development of a closed-type 4c air suspension leveling logic," *Technical Journal of Hyundai Mobis*, vol. 9, p. 2, 2008.
- [4] X. Li, S. Zheng, J. Zhang, and K. Li, "Modelling and simulation study on application of sliding-mode control for an active anti-roll system in a passenger car with air suspension," *International journal of vehicle design*, vol. 49, pp. 318-337, 2009.
- [5] I. Jang, H. Kim, H. Lee, and S. Han, "Height control and failsafe algorithm for closed loop air suspension control system," *International Conference on Control, Automation and Systems*, 2007, pp. 373-378.

- [6] H. Kim, H. Lee, and H. Kim, "Asynchronous and synchronous load leveling compensation algorithm in airspring suspension," *International Conference on Control, Automation and Systems*, 2007, pp. 367-372.
- [7] D. R. Tener, "Overcoming the Ride/Handling Compromise-A Cockpit Adjustable Suspension System," SAE Technical Paper 0148-7191, 2004.
- [8] J. Braun, "Race Track Development of a Hydraulic Ride Height Control System," SAE Technical Paper 0148-7191, 1996.
- [9] C. Giliomee and P. Els, "Semi-active hydropneumatic spring and damper system," *Journal of Terramechanics*, vol. 35, pp. 109-117, 1998.
- [10] M. Hiruma, "Vehicle hydropneumatic suspension system with vehicle body height control means," ed: Google Patents, 1978.
- [11] S. B. Shukhman and V. E. Malyarevich, "Making Greener Off-Road Vehicles- Assessment Method and Design Solutions," SAE Technical Paper 0148-7191, 2011.
- [12] M. Van Damme, B. Vanderborght, R. Van Ham, B. Verrelst, F. Daerden, and D.

Lefeber, "Sliding Mode Control of a 2DOF Planar Pneumatic Manipulator," *Journal of Dynamic Systems, Measurement, and Control*, vol. 131, p. 021013, 2009.

[13] K. Ahn and S. Yokota, "Intelligent switching control of pneumatic actuator using on/off solenoid valves," *Mechatronics*, vol. 15, pp. 683-702, 2005.

[14] H. I. Ali, S. B. B. M. Noor, S. Bashi, and M. Marhaban, "A review of pneumatic actuators (modeling and control)," *Australian Journal of Basic and Applied Sciences*, vol. 3, pp. 440-454, 2009.

[15] H. Schulte and H. Hahn, "Fuzzy state feedback gain scheduling control of servo-pneumatic actuators," *Control Engineering Practice*, vol. 12, pp. 639-650, 2004.

[16] M. Smaoui, X. Brun, and D. Thomasset, "A study on tracking position control of an electropneumatic system using backstepping design," *Control Engineering Practice*, vol. 14, pp. 923-933, 2006.

[17] M. Smaoui, X. Brun, and D. Thomasset, "Systematic control of an electropneumatic system: integrator backstepping and sliding mode control," *IEEE Transactions on Control Systems Technology*, vol. 14, pp. 905-913, 2006.

- [18] T. Nguyen, J. Leavitt, F. Jabbari, and J. Bobrow, "Accurate sliding-mode control of pneumatic systems using low-cost solenoid valves," *IEEE/ASME Transactions on Mechatronics*, vol. 12, pp. 216-219, 2007.
- [19] B. Surgenor and N. Vaughan, "Continuous sliding mode control of a pneumatic actuator," *Journal of dynamic systems, measurement, and control*, vol. 119, pp. 578-581, 1997.
- [20] H. Kim and H. Lee, "Height and leveling control of automotive air suspension system using sliding mode approach," *IEEE Transactions on Vehicular Technology*, vol. 60, pp. 2027-2041, 2011.
- [21] X. Xu, L. Chen, L. Sun, and X. Sun, "Dynamic ride height adjusting controller of ECAS vehicle with random road disturbances," *Mathematical Problems in Engineering*, vol. 2013, 2013.

APPENDIX I: WORK BREAKDOWN

